

1 **Title**

2

3 On the design of CRISPR-based single cell molecular screens

4

5 **Authors**

6

7 Andrew J. Hill<sup>1,\*</sup>, José L. McFaline-Figueroa<sup>1,\*</sup>, Lea M. Starita<sup>1</sup>, Molly J. Gasperini<sup>1</sup>, Kenneth  
8 A. Matreyek<sup>1</sup>, Jonathan Packer<sup>1</sup>, Dana Jackson<sup>1</sup>, Jay Shendure<sup>1,2,†</sup>, Cole Trapnell<sup>1,†</sup>

9

10 <sup>1</sup> Department of Genome Sciences, University of Washington, Seattle, WA, USA

11 <sup>2</sup> Howard Hughes Medical Institute, Seattle, WA, USA

12

13 \* These authors contributed equally to this work

14 † These authors contributed equally to this work

15

16 Correspondence to [colettrap@uw.edu](mailto:colettrap@uw.edu) (CT) & [shendure@uw.edu](mailto:shendure@uw.edu) (JS)

## 17 Abstract

18  
19 Several groups recently reported coupling CRISPR/Cas9 perturbations and single cell RNA-seq  
20 as a potentially powerful approach for forward genetics. Here we demonstrate that vector designs  
21 for such screens that rely on *cis* linkage of guides and distally located barcodes suffer from  
22 swapping of intended guide-barcode associations at rates approaching 50% due to template  
23 switching during lentivirus production, greatly reducing sensitivity. We optimize a published  
24 strategy, CROP-seq, that instead uses a Pol II transcribed copy of the sgRNA sequence itself,  
25 doubling the rate at which guides are assigned to cells to 94%. We confirm this strategy performs  
26 robustly and further explore experimental best practices for CRISPR/Cas9-based single cell  
27 molecular screens.

## 28 Introduction

29  
30  
31 Forward genetic screens in cell culture, based on RNA interference or CRISPR/Cas9, enable the  
32 functional characterization of thousands of programmed perturbations in a single experiment<sup>1,2</sup>.  
33 However, the options for phenotypic assays that are compatible with such screens are often  
34 limited to coarse phenotypes such as relative cell growth or survival, and moreover are  
35 uninformative with respect to the mechanism by which each positively scoring perturbation  
36 mediates its effect.

37  
38 To circumvent these limitations, several groups recently reported using single cell RNA-seq  
39 (scRNA-seq)<sup>3-5</sup> as a readout for CRISPR-Cas9 forward genetic screens, *i.e.* to broadly capture  
40 phenotypic effects at the molecular level. A key aspect of these methods is that the guide RNA  
41 (sgRNA) present in each single cell is identified together with its transcriptome, either by means  
42 of a Pol II transcribed barcode that is linked *in cis* to the sgRNA (CRISP-seq, Perturb-Seq,  
43 Mosaic-seq<sup>6-9</sup>) (**Fig. 1a**), or alternatively by capturing the sgRNA sequence itself as part of an  
44 overlapping Pol II transcript (CROP-seq<sup>10</sup>) (**Fig. 1b**).

45  
46 In our own efforts to develop similar methods, we have encountered several important technical  
47 challenges not yet fully delineated in the literature. First, we have quantified the impact of  
48 template switching during lentiviral packaging on designs that rely on *cis* pairing of each sgRNA  
49 with a distally located barcode, and observed swapping of guide-barcode associations at a rate  
50 approaching 50%. Second, we have coupled targeted sgRNA amplification<sup>7,8</sup> and the published  
51 vector of CROP-seq<sup>10</sup>, and shown that our improved protocol is a robust design for scRNA-seq  
52 readout of CRISPR-based forward genetic screens. Finally, we have tested an attractive  
53 alternative design to CROP-seq, but find it does not result in robust inhibition or editing.

54  
55

## 56 Results

57  
58 We initially pursued a design similar to recently published methods<sup>6-9</sup> in which each sgRNA was  
59 linked to a Pol II transcribed barcode located several kilobases away on the lentiviral construct  
60 (**Fig. 1a**). In our vector (pLGB-scKO), the barcode was positioned in the 3' UTR of a blasticidin  
61 resistance transgene, such that it could be recovered by scRNA-seq methods that prime off of  
62 poly(A) tails (**Fig. S1a-b**). Guides and barcodes were paired during DNA synthesis, which  
63 facilitated pooled cloning and lentiviral delivery (**Fig. S1c**).  
64

65 With this design, we sought to ask how loss-of-function (LoF) of various tumor suppressors  
66 altered the transcriptional landscape of immortalized, non-transformed breast epithelial cells<sup>11</sup>.  
67 Specifically, we targeted *TP53* and other tumor suppressors in the MCF10A cell line, with or  
68 without exposure to doxorubicin, which induces double-strand breaks (DSBs) and a  
69 transcriptional response to DNA damage. Cloning and lentiviral packaging was either performed  
70 individually for each targeted gene, or in a pooled fashion. In addition to scRNA-seq, we  
71 performed targeted amplification to more efficiently recover the sgRNA-linked barcodes present  
72 in each cell (**Fig. S1b**; **Fig. S2**).  
73

74 In a first experiment in which a small number of lentiviral constructs were cloned and packaged  
75 separately for each gene ('arrayed lentiviral production'), a substantial proportion of cells in  
76 which *TP53* was targeted had a gene expression signature consistent with a failure to activate a  
77 cell cycle checkpoint response after DNA damage, in line with *TP53*'s pivotal role in this  
78 pathway (*e.g.* lower expression of *CDKN1A* and *TP53I3*; **Fig. S3a**). However, these effects were  
79 greatly reduced when we performed a similar experiment with pooled cloning and lentiviral  
80 packaging (**Fig. S3b**). Furthermore, markedly fewer genes were differentially expressed across  
81 the targets in the pooled experiment than in the arrayed experiment (**Fig. S3c**).  
82

83 Based on what is known about HIV, we reasoned that template switching during pooled  
84 packaging of lentivirus could result in the integration of constructs where the designed  
85 sgRNA-barcode pairings are partially randomized. During viral production, lentiviral plasmids  
86 are transfected into HEK293T cells at high copy number and transcribed<sup>12</sup>. Lentiviral virions are  
87 pseudodiploid, meaning that two viral transcripts are co-packaged within each virion<sup>13</sup>. The  
88 reverse transcriptase that performs negative strand synthesis has a remarkably high rate of  
89 template switching<sup>14</sup>, estimated as roughly 1 event per kilobase (kb)<sup>15</sup>. Template switching would  
90 be expected to result in the integration of chimeric products at a rate proportional to the distance  
91 between paired sequences, effectively swapping intended sgRNA-barcode associations (**Fig. 1c**).  
92 This risk was noted by Adamson et al.<sup>7</sup> and Dixit et al.<sup>8</sup>. It was also altogether avoided by  
93 Adamson et al.<sup>7</sup> through arrayed lentiviral production, but pooled lentiviral production was  
94 performed in some or all experiments of the other reports<sup>6,8,9</sup>. Although Sack et al.<sup>16</sup> recently

95 quantified this phenomenon at distances up to 720 bp in vectors designed for bulk selection  
96 screens, the implications of template switching at longer distances (e.g., the 2.5 kb+ separation  
97 between sgRNAs and barcodes in the pLGB-scKO, CRISP-seq, Perturb-seq, and Mosaic-seq  
98 vectors), as well as for scRNA-seq study designs specifically, remain unexplored. Given a large  
99 enough distance between the barcode and the sgRNA, *cis* linkage between the two sequences  
100 would be lost in ~50% of integration events (an odd number of template switching events) and  
101 maintained in ~50% (an even number of template switching events).

102  
103 To quantify the extent of swapping between two distally located sequences during lentiviral  
104 packaging, we cloned BFP and GFP transgenes, which differ by three base pairs, into separate  
105 lentiviral vectors (pHAGE-GFP and pHAGE-BFP). We paired each transgene with a unique  
106 barcode, separated from the nearest unique bases in BFP/GFP by 2.4 kb (**Fig. 1d**) to approximate  
107 the 2.5 kb or greater separation between sgRNAs and barcodes in the pLGB-scKO, CRISP-seq,  
108 Perturb-Seq, and Mosaic-seq vectors<sup>6-9</sup>. We then transduced MCF10A cells with lentivirus  
109 generated either individually or as a pool of the two plasmids. Finally, we sorted GFP+ or BFP+  
110 fractions of the cells with FACS, and quantified the rate of barcode swapping (**Fig. 1e; Fig. S4**).  
111 At this distance, *cis* linkage is lost at the theoretical maximum rate of 50% (**Fig. 1f; Fig. S5**). Our  
112 observations are consistent with previous estimates of template switching in HIV<sup>15</sup> and recent  
113 studies in lentivirus at distances below 1 kb<sup>16</sup>.

114  
115 In order to simulate the impact of template switching, we obtained data from a pilot experiment  
116 of Adamson *et al.*<sup>7</sup> generated using the Perturb-seq vector with arrayed lentiviral production,  
117 targeting several transcription factors with CRISPRi. We swapped target labels *in silico* in these  
118 data at varying rates, and evaluated the impact on power to detect differential expression. At a  
119 50% swap rate, we observe a 4.8-fold decrease in the number of differentially expressed genes  
120 (**Fig. 1g**). This loss in power results from an effective reduction of the useful sample size for  
121 each target by twofold and contamination of each target with noise from swapped associations,  
122 thus shifting all targets towards the population average of the library.

123  
124 One of the published strategies for CRISPR-based single cell molecular screens, CROP-seq<sup>10</sup>,  
125 does not rely on pairing of sgRNAs and barcodes. Instead, the sequence of the integrated sgRNA  
126 itself acts as a barcode, as part of an overlapping Pol II transcript. In addition, the sgRNA  
127 cassette is copied from the 3' to 5' LTR during positive strand synthesis (**Fig. 1b**). This copy is  
128 generated during an intramolecular priming step that does not result in intermolecular swapping  
129 at an appreciable rate<sup>17</sup>. A limitation of the CROP-seq method as described is that the sgRNA  
130 expressed in each cell is recovered as part of its transcriptome with limited sensitivity  
131 (~40-60%)<sup>10</sup>. The roughly half of single cell transcriptomes for which the sgRNA is not  
132 identified are discarded. To improve upon this, we modified the CROP-seq protocol to include



133 targeted amplification of the sgRNA region from mRNA libraries that have already been tagged  
134 with cellular barcodes, as in our initial pLGB-scKO design (**Fig. 2a; Fig. S6**).

135  
136 To evaluate the effectiveness of this approach, we performed a CRISPR-mediated LoF screen of  
137 32 tumor suppressors (6 guides per target) and 6 non-targeting control (NTC) guides in MCF10A  
138 cells with or without exposure to doxorubicin. Whereas the sgRNA was identified in the shotgun  
139 transcriptome of only 42-47% of cells, it was identified in 94% of cells with targeted  
140 amplification (**Fig. 2b**). In sharp contrast with our original pooled experiment that also targeted  
141 TP53, a tSNE embedding of doxorubicin-exposed cells from this experiment yielded a cluster  
142 that is almost entirely composed of cells containing TP53-targeting sgRNAs, highlighting the  
143 unique molecular phenotype imparted by TP53 loss when responding to DSBs (**Fig. 2c**).  
144 Specifically, the 262 cells in this cluster include 90.5% with TP53-targeting guides, 7.6% with  
145 guides targeting other genes, 0% with NTC guides, and 1.9% that were unassigned. In contrast,  
146 the remaining 5,617 cells included 3.2% with TP53-targeting guides (presumably cells in which  
147 editing failed to occur, or in which editing maintained a functional protein), 84.2% with guides  
148 targeting other genes, 7.5% with NTC guides, and 5.2% that were unassigned. Expression levels  
149 of the p53 targets *CDKN1A* and *TP53I3*<sup>18,19</sup> were markedly lower in the TP53-targeted cluster  
150 (**Fig. 2d**), and 4,277 and 2,186 differentially expressed genes (FDR 5%) were identified relative  
151 to cells with NTC guides in the doxorubicin-treated and mock condition, respectively. The clean  
152 separation between the TP53-targeted cluster and other cells is presumably a consequence of: (a)  
153 the large effect of knocking out TP53; (b) our ability to recover sgRNA labels in a nearly all cells  
154 via targeted amplification; (c) the lack of sgRNA/barcode swapping, because of CROP-seq; (d)  
155 the high efficiency of CROP-seq expressed sgRNA in mediating nonhomologous end-joining.

156  
157 Upon applying dimensionality reduction and clustering to cells in both the mock and doxorubicin  
158 treated conditions (**Fig. S7a-b**), we find several other tumor suppressors whose distribution  
159 across tSNE clusters is significantly different compared to NTCs (FDR 5%), with more changes  
160 observed after doxorubicin exposure (**Fig. S7c-f**). To characterize clusters in which we observe  
161 enrichment of particular targets, we tested for target enrichment within clusters and generated  
162 average expression profiles for each enriched target-cluster pair. Gene set enrichment analysis of  
163 the most highly loaded genes in the principal components of these average expression profiles  
164 show many targets to be associated with increased proliferation and a decreased TP53/DNA  
165 damage response, with the extent of this effect being largest for TP53 (**Fig. S8**).

166  
167 To further assess the impact of lentivirus template switching would have on sensitivity, we  
168 permuted target labels at varying rates within our own CROP-seq tumor suppressor screen and  
169 find a 2.9-fold reduction in the number of DEGs observed across the targets at a swap rate of  
170 50%. Enrichment tests on our tumor suppressor screen with a 50% simulated swap rate  
171 substantially decreased the number of knockouts that display a significant change in phenotype

172 in both mock and doxorubicin treated conditions, recovering just 4/13 (*TP53*, *STK11*, *CHEK1*  
173 and *NCOR1*) and 3/14 (*TP53*, *RBI*, and *ARID1B*) targets as enriched in the mock and  
174 doxorubicin conditions, respectively. Additionally, swapping simulations on the much larger  
175 (50,000 cells) unfolded protein response screen from Adamson *et al.* with arrayed lentiviral  
176 production show a 1.9- and 2.8-fold reduction at a simulated swap rate of 50% when using  
177 25,000 and 6,000 cells, respectively (**Fig. S9**). These simulations demonstrate that the effect of  
178 barcode-sgRNA pair swapping is dependent on the number of cells captured and also on  
179 sequencing depth, number of targets examined and the effect size for those targets.

180  
181 Although the CROP-seq design is not subject to sgRNA-barcode swapping, it is potentially  
182 limited by its placement of the sgRNA cassette in the LTR of the lentiviral vector, as larger  
183 intervening sequences may render the LTR non-functional<sup>10</sup>. To enable incorporation of longer  
184 cassettes, such as dual sgRNA designs<sup>20-22</sup>, we sought to place the sgRNA cassette between the  
185 WPRE and LTR. In this design (pHAGE-scKO), a second copy of this cassette would not be  
186 generated. However, the guide sequence would still contribute to overlapping Pol II and Pol III  
187 transcripts; for the former, it is positioned to ensure its incorporation into the 3' end of the  
188 blasticidin resistance gene (**Fig. 2e**).

189  
190 To evaluate this design, we compared the ability of pHAGE-scKO, CROP-seq, and a standard  
191 lentiviral sgRNA expression vector, pKHH030<sup>23</sup>, all containing a CRISPRi optimized backbone,  
192 to inhibit transcription via CRISPRi. We targeted the promoter of lentivirally-integrated mCherry  
193 in both MCF10A and K562 cells, which were then assayed for fluorescence via FACS. Whereas  
194 pKHH030 and CROP-seq exhibited efficient inhibition of mCherry, pHAGE-scKO had poor  
195 efficacy in both cell lines (**Fig. 2f**). Consistent with this, we observed low editing rates with our  
196 new design in MCF10A cells (88% edited with pLGB control vs. 29% edited with  
197 pHAGE-scKO). Recent studies have hinted at interference when Pol II and Pol III transcripts  
198 overlap<sup>24,25</sup>. We hypothesize that the observed decrease in editing and inhibition efficiency of the  
199 pHAGE-scKO design is due to the blasticidin resistance gene (Pol II promoter) inhibiting  
200 expression of the Pol III sgRNA. In contrast, CROP-seq likely maintains efficacy because the  
201 second integrated copy of the guide expression cassette (copied to the 5' LTR during positive  
202 strand synthesis) does not overlap a Pol II transcript.

## 203 204 **Discussion**

205  
206 CRISPR-based forward genetic screens that rely on scRNA-seq to phenotype each perturbation  
207 have the potential to be extremely powerful. However, as we demonstrate here, there are  
208 important technical considerations that must be taken into account. Several published designs, as  
209 well as our own initial design (pLGB-scKO), suffer from high rates (50%) of swapped  
210 sgRNA-barcode associations, consequent to template switching across the several kilobases

211 between the sgRNA and barcode during lentiviral production. Importantly, we do not expect that  
212 positive conclusions drawn by published studies utilizing such designs in conjunction with  
213 pooled lentivirus production<sup>6,8,9</sup> are incorrect. Each of these studies examined a small number of  
214 targets and collected large datasets ranging from 25,000 to 100,000 cells per screen with ample  
215 sequencing depth, raising their baseline sensitivity. However, given the high cost of single-cell  
216 capture and sequencing and the need to expand the number of targets in such screens, our  
217 observation of ~50% swapping of sgRNA-barcode associations with pooled lentiviral production  
218 using vectors in which the sgRNA and barcode are separated by several Kb, are highly relevant  
219 for ongoing and future studies. This loss of power may be overcome in part by filtering cells that  
220 appear inconsistent with their assigned knock-out<sup>8</sup>, or overcome altogether by performing  
221 cloning and lentiviral packaging separately for guides targeting each gene<sup>7</sup>. However,  
222 computational filtering of cells has the potential to introduce biases, and itself reduces power by  
223 discarding collected data, while performing cloning and lentiviral packaging separately for each  
224 sgRNA dramatically limits scalability.

225  
226 We also explored an alternative design (pHAGE-scKO), that like CROP-seq allows sequencing  
227 of the sgRNA sequence directly, in hopes that it would facilitate the use of dual guide RNAs or  
228 other designs that require longer cassettes. However, we observe markedly reduced  
229 editing/inhibition with this design. It is plausible that methods such as programmed multiplexed  
230 guide expression cassettes<sup>20-22,26</sup> could be used in conjunction with CROP-seq due to their  
231 reduced length, but it will be important to carefully validate any such designs.

232  
233 As the community increasingly adopts scRNA-seq as a readout for forward genetic screens, we  
234 believe that each of these technical hurdles merit careful consideration. By coupling targeted  
235 sgRNA amplification and the published CROP-seq method<sup>10</sup>, we doubled the proportion of cells  
236 in which guides are assigned to cells, to 94%. The attractive features of this approach include the  
237 simplicity of the cloning protocol, its compatibility with lentiviral delivery, the high rate of  
238 recovery of sgRNA-cell associations, and no risk of template switching.

## 239 **Acknowledgements**

240  
241  
242 We thank all members of the Shendure and Trapnell labs for feedback on our manuscript and  
243 helpful discussions, particularly Sanjay Srivatsan, Greg Findlay, Aaron McKenna, Riza Daza,  
244 Beth Martin, Martin Kircher, Darren Cusanovich, Xiaojie Qiu, and Vijay Ramani. We thank  
245 Professors Jesse Bloom and Douglas Fowler for discussions about lentivirus; Dr. Kyuho Han,  
246 James Ousey, and Professor Mike Bassik for experimental advice and reagents for CRISPRi  
247 experiments. AH thanks Stella the cat for support. This work was supported by the following  
248 funding: NIH DP1HG007811 and UM1HG009408 (to JS), DP2HD088158 (to CT), and the W.  
249 M. Keck Foundation (to CT and JS). AH and MG are funded by the National Science Foundation

250 Graduate Research Fellowship. JLM is supported by the NIH Genome Training Grant  
251 (5T32HG000035) and the Cardiovascular Research Training Grant (4T32HL007828). CT is  
252 partly supported by an Alfred P. Sloan Foundation Research Fellowship. JS is an Investigator of  
253 the Howard Hughes Medical Institute.

254

255

#### 256 **Data availability.**

257 Data is available on GEO via accession GSE108699 and code along with additional data are  
258 available on Github as described below. pHAGE-GFP, pHAGE-BFP, and the CROP-seq vector  
259 with the CRISPRi-optimized backbone sequence described in methods are available on Addgene  
260 as 106281, 106282, and 106280, respectively (currently pending). The CROP-seq vector with the  
261 standard backbone was used as described in Datlinger *et. al* (see methods).

262

#### 263 **Code Availability**

264 Code for useful scripts and analysis from the paper, more details on data access (as mentioned  
265 above), and 10X V2 enrichment PCR details are available at:  
266 <https://github.com/shendurelab/single-cell-ko-screens>.

267

#### 268 **References**

269

1. Shalem, O., Sanjana, N. E. & Zhang, F. High-throughput functional genomics using  
270 CRISPR–Cas9. *Nat. Rev. Genet.* **16**, 299–311 (2015).
2. Mohr, S. E., Smith, J. A., Shamu, C. E., Neumüller, R. A. & Perrimon, N. RNAi screening  
271 comes of age: improved techniques and complementary approaches. *Nat. Rev. Mol. Cell*  
272 *Biol.* **15**, 591–600 (2014).
- 273 3. Macosko, E. Z. *et al.* Highly Parallel Genome-wide Expression Profiling of Individual Cells  
274 Using Nanoliter Droplets. *Cell* **161**, 1202–1214 (2015).
- 275 4. Klein, A. M. *et al.* Droplet barcoding for single-cell transcriptomics applied to embryonic  
276 stem cells. *Cell* **161**, 1187–1201 (2015).
- 277 5. Zheng, G. X. Y. *et al.* Massively parallel digital transcriptional profiling of single cells. *Nat.*  
278 *Commun.* **8**, 14049 (2017).
- 279

- 280 6. Xie, S., Duan, J., Li, B., Zhou, P. & Hon, G. C. Multiplexed Engineering and Analysis of  
281 Combinatorial Enhancer Activity in Single Cells. *Mol. Cell* **66**, 285–299.e5 (2017).
- 282 7. Adamson, B. *et al.* A Multiplexed Single-Cell CRISPR Screening Platform Enables  
283 Systematic Dissection of the Unfolded Protein Response. *Cell* **167**, 1867–1882.e21 (2016).
- 284 8. Dixit, A. *et al.* Perturb-Seq: Dissecting Molecular Circuits with Scalable Single-Cell RNA  
285 Profiling of Pooled Genetic Screens. *Cell* **167**, 1853–1866.e17 (2016).
- 286 9. Jaitin, D. A. *et al.* Dissecting Immune Circuits by Linking CRISPR-Pooled Screens with  
287 Single-Cell RNA-Seq. *Cell* **167**, 1883–1896.e15 (2016).
- 288 10. Datlinger, P. *et al.* Pooled CRISPR screening with single-cell transcriptome readout. *Nat.*  
289 *Methods* **14**, 297–301 (2017).
- 290 11. Debnath, J., Muthuswamy, S. K. & Brugge, J. S. Morphogenesis and oncogenesis of  
291 MCF-10A mammary epithelial acini grown in three-dimensional basement membrane  
292 cultures. *Methods* **30**, 256–268 (2003).
- 293 12. Tseng, W. C., Haselton, F. R. & Giorgio, T. D. Transfection by cationic liposomes using  
294 simultaneous single cell measurements of plasmid delivery and transgene expression. *J.*  
295 *Biol. Chem.* **272**, 25641–25647 (1997).
- 296 13. Nikolaitchik, O. A. *et al.* Dimeric RNA recognition regulates HIV-1 genome packaging.  
297 *PLoS Pathog.* **9**, e1003249 (2013).
- 298 14. Jetzt, A. E. *et al.* High rate of recombination throughout the human immunodeficiency virus  
299 type 1 genome. *J. Virol.* **74**, 1234–1240 (2000).
- 300 15. Schlub, T. E., Smyth, R. P., Grimm, A. J., Mak, J. & Davenport, M. P. Accurately measuring  
301 recombination between closely related HIV-1 genomes. *PLoS Comput. Biol.* **6**, e1000766

- 302 (2010).
- 303 16. Sack, L. M., Davoli, T., Xu, Q., Li, M. Z. & Elledge, S. J. Sources of Error in Mammalian  
304 Genetic Screens. *G3* **6**, 2781–2790 (2016).
- 305 17. Yu, H., Jetzt, A. E., Ron, Y., Preston, B. D. & Dougherty, J. P. The nature of human  
306 immunodeficiency virus type 1 strand transfers. *J. Biol. Chem.* **273**, 28384–28391 (1998).
- 307 18. el-Deiry, W. S. *et al.* WAF1, a potential mediator of p53 tumor suppression. *Cell* **75**,  
308 817–825 (1993).
- 309 19. Contente, A., Dittmer, A., Koch, M. C., Roth, J. & Dobbstein, M. A polymorphic  
310 microsatellite that mediates induction of PIG3 by p53. *Nat. Genet.* **30**, 315–320 (2002).
- 311 20. Gasperini, M. *et al.* CRISPR/Cas9-Mediated Scanning for Regulatory Elements Required  
312 for HPRT1 Expression via Thousands of Large, Programmed Genomic Deletions. *Am. J.*  
313 *Hum. Genet.* **101**, 192–205 (2017).
- 314 21. Diao, Y. *et al.* A tiling-deletion-based genetic screen for cis-regulatory element  
315 identification in mammalian cells. *Nat. Methods* **14**, 629–635 (2017).
- 316 22. Vidigal, J. A. & Ventura, A. Rapid and efficient one-step generation of paired gRNA  
317 CRISPR-Cas9 libraries. *Nat. Commun.* **6**, 8083 (2015).
- 318 23. Han, K. *et al.* Synergistic drug combinations for cancer identified in a CRISPR screen for  
319 pairwise genetic interactions. *Nat. Biotechnol.* **35**, 463–474 (2017).
- 320 24. Lukoszek, R., Mueller-Roeber, B. & Ignatova, Z. Interplay between polymerase II- and  
321 polymerase III-assisted expression of overlapping genes. *FEBS Lett.* **587**, 3692–3695  
322 (2013).
- 323 25. Yeganeh, M., Praz, V., Cousin, P. & Hernandez, N. Transcriptional interference by RNA



- 324 polymerase III affects expression of the Polr3e gene. *Genes Dev.* **31**, 413–421 (2017).
- 325 26. Zhu, S. *et al.* Genome-scale deletion screening of human long non-coding RNAs using a  
326 paired-guide RNA CRISPR-Cas9 library. *Nat. Biotechnol.* **34**, 1279–1286 (2016).
- 327 27. Sanjana, N. E., Shalem, O. & Zhang, F. Improved vectors and genome-wide libraries for  
328 CRISPR screening. *Nat. Methods* **11**, 783–784 (2014).
- 329 28. Chen, B. *et al.* Dynamic imaging of genomic loci in living human cells by an optimized  
330 CRISPR/Cas system. *Cell* **155**, 1479–1491 (2013).
- 331 29. McKenna, A. *et al.* Whole-organism lineage tracing by combinatorial and cumulative  
332 genome editing. *Science* **353**, aaf7907 (2016).
- 333 30. Dixit, A. Correcting Chimeric Crosstalk in Single Cell RNA-seq Experiments. (2016).  
334 doi:10.1101/093237
- 335 31. Qiu, X. *et al.* Single-cell mRNA quantification and differential analysis with Census. *Nat.*  
336 *Methods* **14**, 309–315 (2017).

## 337 **Methods**

### 338 ***Cell Lines and Culture***

339 MCF10A immortalized breast epithelial cells were purchased from ATCC and cultured in  
340 DMEM/F12 (Invitrogen) supplemented with 10% FBS, 1% penn-strep, 10 ng/mL EGF, 1 µg/mL  
341 hydrocortisone, 5 µg/mL insulin and 100 ng/mL cholera toxin.

342

### ***Generating an Inducible Cas9 Expressing MCF10A Cell Line***

343 Lentivirus containing a doxycycline inducible and constitutively expressed Cas9 construct was  
344 produced by transfecting 293T cells with either pCW-Cas9 (Addgene #50661) or lentiCas9-Blast  
345 (Addgene #52962) and plasmids from the ViraPower Lentiviral Expression System (Thermo)  
346 according to manufacturer's instructions. 48 hours post transfection, virus containing supernatant  
347 was collected and cell debris removed by filtering through a 40 µm syringe filter. MCF10A cells  
348 were transduced with filtered supernatant for 48 hours and selected with 1 µg/mL puromycin



349 (pCW-Cas9) or 10 µg/mL blasticidin (lentiCas9-Blast) for 96 hours. For cells expressing a  
350 doxycycline inducible Cas9 single cell clones of MCF10A-Cas9 cells were generated by high  
351 rate of dilution, individual clones expanded and Cas9 expression of individual clones was  
352 confirmed by immunoblotting of cells 96 hours following addition of doxycycline at 1  
353 microgram/mL. lentiCas9-Blast cells were maintained as a polyclonal line.

354  
355 pCW-Cas9 cells were used for initial arrayed and pooled screens, as well as quantification of  
356 editing rates in pHAGE-scKO vector. lentiCas9-Blast cells were used for all CROP-seq  
357 experiments.

358

### ***Initial Tagged Transcript Cloning Method***

359 Due to our results demonstrating high rates of barcode/sgRNA swapping when using this design,  
360 we do not recommend use of this protocol.

361

362 Starting with the standard lentiGuide-puro plasmid (Addgene #52963), this vector was modified  
363 to confer blasticidin resistance, a mechanism of selection independent from the pCW-Cas9 (puro  
364 resistance) plasmid used to generate MCF10A-Cas9 cells. Puro and its EF-1A promoter were  
365 removed via a double digest with NEB SmaI (8 hours at 25 degrees C) and MLU1-HF (8 hours  
366 25 degrees C). This product was gel purified using QiaQuick Gel Extraction kit (Qiagen). EF-1A  
367 promoter and Blasticidin, each with 20 bp homology on both ends were prepared via PCR from  
368 lentiCas9-Blast and gel purified. Fragments were assembled into digested lentiGuide-puro vector  
369 using the NEBuilder HiFi DNA Assembly kit with inserts in 2-fold molar excess and  
370 transformed into NEB C3040H E. Coli and allowed to incubate overnight at 30 degrees C.  
371 Clones were picked from plate, allowed to grow in LB+amp overnight at 30 degrees, and were  
372 purified using Qiagen Miniprep kit. Individual clones were validated via Sanger sequencing.

373

374 Lentiguide-blast was linearized using a digest with BsmB1 (Thermo) at 37 degrees for five hours  
375 followed by digestion with Sali HF (NEB) overnight and gel purification. Oligos containing both  
376 guide sequences and their corresponding barcodes were designed according to the following:

377 tGTGGAAAGGACGAAACACC[G][guide]gttttagagctaGAAAtagcagagacgCGTCTCAgatatccctt  
378 tgggccgctccccgcg[barcode]tcgactttaagaccaatgacttaca

379

380 Where [guide] is a 20 bp guide sequence and [barcode] is an 8 bp barcode sequence uniquely  
381 paired to a particular sgRNA. Note that the [G] included prior to the guide is required for  
382 expression from a Pol III promoter. Guides that generate an extra BsmB1 restriction site when  
383 used in this design were excluded due to incompatibility with our downstream cloning strategy  
384 and only barcode sequences that did not generate additional BsmB1 restriction sites were used.  
385 RUNX1 was the only target impacted by this filter (4 guides were used instead of 6).

386  
387 A library of these oligos was ordered in 96 well format as Ultramers from Integrated DNA  
388 Technologies and resuspended at equal molarity. All oligos were resuspended in water, pooled at  
389 equimolar concentrations, and amplified using a 50 microliter PCR KAPA HiFi HotStart Ready  
390 Mix PCR reaction with 1 ng of input DNA, an annealing temperature of 62 degrees, an extension  
391 time of 20 seconds, and all other parameters according to the manufacturer's recommendations.  
392 The resulting product was cleaned with a Zymo DNA Clean and Concentrator kit. The purified  
393 inserts were assembled into linearized lentiGuide-blast using the NEBuilder HiFi DNA  
394 Assembly kit and a molar excess of 1:5 vector to insert ratio. Assembled products were  
395 transformed into NEB C3040H E. Coli and grown overnight at 30 degrees in LB+amp. Product  
396 was prepared using a plasmid Miniprep kit (Qiagen).

397  
398 To prepare the insert for the final reaction, a region spanning from the backbone sequence for the  
399 CRISPR sgRNA to a region towards the end of the WPRE element was amplified using the  
400 KAPA HiFi Hotstart Master Mix and purified using the Zymo Clean and Concentrator kit. The  
401 primers used in this reaction add BsmB1 cut sites that generate complementary ends in the final  
402 cloning step following digestion. This amplified fragment was ligated into PGEM-T following  
403 the kit protocol and a clone was selected via blue-white screening and validation of individual  
404 clones by Sanger sequencing. The validated construct was digested with BsmB1 (Thermo) and  
405 gel purified.

406  
407 The fragment isolated from PGEM-T was then ligated into this linearized vector using a 3:1  
408 molar excess of insert to vector using T4 DNA Ligase (New England Biolabs) and a an overnight  
409 incubation at 16 degrees C. Ligation products were transformed into NEB C3040H (stable)  
410 competent cells and grown overnight at 30 degrees in LB+amp. Plasmids were recovered using  
411 a Plasmid Miniprep kit (Qiagen).

412  
***pHAGE Vector Cloning***  
413 The pHAGE\_dsRed\_IRES\_zsGreen vector was modified to contain a multiple cloning site as  
414 described in *Quantification of Template Switching in Lentivirus Packaging Using FACS*. The  
415 U6-sgRNA cassette containing a 500bp filler removable by BsmB1 digest was ordered as a  
416 gblock (Integrated DNA Technologies). Using the multiple cloning site, the U6-sgRNA cassette  
417 was added in the three-prime UTR of the zsGreen/dsRed transgene via Gibson assembly. This  
418 vector was further modified to remove the zsGreen/IRES/dsRed cassette and replace the CMV  
419 promoter with an EF1a promoter.

420  
421 The vector was digested following the protocol outlined in Sanjana and Shalem *et al.*<sup>27</sup>. Oligos  
422 corresponding to individual guides with homology for gblock assembly were ordered as standard

423 DNA oligos in 96-well plate format from Integrated DNA Technologies with the following  
424 design:

425  
426 [GCCTTATTTTAACTTGCTATTTCTAGCTCTAAAAC][GUIDE  
427 RC][C][GGTGTTCGTCCTTTCCACAAGAT]

428  
429 Guide RC refers to the reverse complement of the guide sequence. The entire construct may also  
430 be reverse complemented, allowing the guide sequence itself to be used rather than the reverse  
431 complement. Note that the additional C included here is required for transcription from the Pol  
432 III promoter.

433  
434 All oligos were resuspended in water, pooled at equimolar concentrations, and amplified using a  
435 50 microliter PCR KAPA HiFi HotStart Ready Mix PCR reaction with 1 ng of input DNA, an  
436 annealing temperature of 62 degrees, an extension time of 20 seconds, and all other parameters  
437 according to the manufacturer's recommendations. The following primers were used for  
438 amplification:

439  
440 Forward: 5 - GCCTTATTTTAACTTGCTATTTCTAGCT - 3  
441 Reverse: 5 - ATCTTGTGGAAAGGACGAAACA - 3

442  
443 Reactions were monitored with qPCR and stopped just prior to saturation.

444  
445 These reactions were cleaned with a Zymo DNA Clean and Concentrator kit and cloned into the  
446 Bsmbl digested pHAGE vector backbone using the Clontech Infusion HD Cloning Kit.  
447 Ligations were performed using 10 fmols of vector and and a 200 fmols of double stranded  
448 oligo (1:20 molar ratio of vector to insert). Ligation products were transformed into NEB  
449 C3040H (stable) cells according to manufacturer recommendations. Transformations were  
450 diluted with 250  $\mu$ L of LB and spread onto 6 LB-AMP plates and incubated at 30 degrees C for  
451 24 hours. Colonies were then scraped into LB, a bacterial pellet was collected and plasmids  
452 recovered using a Plasmid Midiprep kit (Qiagen).

### 453 ***Quantification of Template Switching in Lentivirus Packaging Using FACS***

454 A multiple cloning site was cloned into pHAGE\_dsRed\_IRES\_zsGreen lentiviral vector between  
455 the WPRE and 3'LTR. The multiple cloning site was assembled from annealing and extension of  
456 WPRE\_MCS\_insert\_W and WPRE\_MCS\_insert\_R:

457  
458 WPRE\_MCS\_insert\_W:  
459 5- ctttgggcccctccccgcctgggcccATAACAgctagcTGATGGctcgagcc -3

460  
461 WPRE\_MCS\_insert\_R:  
462 5- cagctgccttgtaagtcattggtcttaaaggctcgagCCATCAgctagcTGTTATgg -3  
463  
464 The plasmid was amplified by inverse PCR with pHAGE\_WPRE\_MCS\_GIBS\_F and R:  
465 pHAGE\_WPRE\_MCS\_GIBS\_F  
466 5- TGGctcgagccttaagaccaatgacttacaagcgagctg -3  
467  
468 pHAGE\_WPRE\_MCS\_GIBS\_R  
469 5- ctagcTGTTATggcgcgccagggcggggaggcggcccaaag -3  
470 The two fragments were cloned by Gibson Assembly. Correct clones of  
471 pHAGE\_dsRed\_IRES\_zsGreen\_WPRE\_MCS were identified by Sanger sequencing and  
472 expression of the fluorescent proteins after transfection and lentiviral packaging.  
473  
474 To make the pHAGE EBFP or EGFP\_IRES\_dsRed\_WPRE\_MCS,  
475 pHAGE\_dsRed\_IRES\_zsGreen\_WPRE\_MCS was cut with BamHI and ClaI to remove the  
476 zsGreen and IRES. The ends were blunted and re-ligated to make pHAGE\_dsRed  
477 \_WPRE\_MCS. EGFP or EBFP (amplified with eGFP\_gibsF and eGFP\_IRES\_GibsR) and an  
478 IRES (IRES\_GibsF, IRES\_GibsR) were cloned into the NotI site 5' of the dsRed, by Gibson  
479 Assembly. EBFP was ordered as a gBlock (Integrated DNA Technologies) with 3 nucleotide  
480 changes from EGFP. Correct clones were identified by sequencing. The dsRed is not expressed  
481 in this construct.  
482  
483 eGFP\_gibsF:  
484 5- gccatccacgctgttttgacctccatagaagacaccggcATGGTGAGCAAGGGCGAGGAG -3  
485  
486 eGFP\_IRES\_GibsR:  
487 5- ggatccCTACTTGTACAGCTCGTCCATGCCG -3  
488  
489 IRES\_GibsF:  
490 5- ATCACTCTCGGCATGGACGAGCTGTACAAGTAGggatccctccccccccctaacgttac -3  
491  
492 IRES\_GibsR:  
493 5- ctcttgatgacgtcctcggaggaggccatggcggccatgtgtggccatattatcatcgtgttttcaaagg -3  
494  
495 EBFP  
496 5-  
497 ATGGTGAGCAAGGGCGAGGAGCTGTTACCGGGGTGGTGCCATCCTGGTTCGAGCT  
498 GGACGGCGACGTAAACGGCCACAAGTTCAGCGTGTCCGGCGAGGGCGAGGGCGATG

499 CCACCTACGGCAAGCTGACCCTGAAGTTCATCTGCACCACCGGCAAGCTGCCCGTGC  
500 CCTGGCCCACCCTCGTGACCACCCTGACCCACGGCGTGCAGTGCTTCAGCCGCTACC  
501 CCGACCACATGAAGCAGCACGACTTCTTCAAGTCCGCCATGCCCGAAGGCTACGTCC  
502 AGGAGCGCACCATCTTCTTCAAGGACGACGGCAACTACAAGACCCGCGCCGAGGTG  
503 AAGTTCGAGGGCGACACCCTGGTGAACCGCATCGAGCTGAAGGGCATCGACTTCAA  
504 GGAGGACGGCAACATCCTGGGGCACAAGCTGGAGTACAACCTtAACAGCCACAACG  
505 TCTATATCATGGCCGACAAGCAGAAGAACGGCATCAAGGTGAACTTCAAGATCCGC  
506 CACAACATCGAGGACGGCAGCGTGCAGCTCGCCGACCACTACCAGCAGAACACCCC  
507 CATCGGCGACGGCCCCGTGCTGCTGCCCGACAACCACTACCTGAGCACCCAGTCCGC  
508 CCTGAGCAAAGACCCCAACGAGAAGCGCGATCACATGGTCCTGCTGGAGTTCGTGA  
509 CCGCCGCCGGGATCACTCTCGGCATGGACGAGCTGTACAAG -3

510  
511 Fifteen nucleotide barcodes (lenti-barcode and lenti-barcode-r) were then cloned into the  
512 multiple cloning site between the WPRE and 3'LTR for both the EBFP and EGFP constructs by  
513 Gibson Assembly. Single clones were prepared and the barcode identified by Sanger sequencing.

514  
515 lenti-barcode:

516 5-  
517 atctcccttgggcccgcctccccgcctgggGGATCCAGNNNNNNNNNNNNNNNNNtcgagccttaagaccaatgactt  
518 acaagg -3

519  
520 lenti-barcode-r:

521 5- CCTTGTAAGTCATTGGTCTTAAAGGCTCGA -3

522  
523 Lentivirus was packaged by transfection of barcoded EGFP or EBFP constructs either alone or in  
524 an equimolar mix along with helper plasmids (pHDM-Hgpm2, pHDM-Tatlb, pRC-CMVRev1b  
525 and pHDM-VSV-G) into HEK293T cells using Lipofectamine 2000 (Invitrogen). Viral  
526 supernatant was collected after 48 hours, spun to remove debris, snap frozen in liquid nitrogen  
527 and stored at -80°C. To titer the packaged lentiviruses, they were thawed on ice and added to  
528 MCF10A cells with media containing 8 micrograms/ml polybrene, and the frequency of  
529 transduced cells 48 hours post-transduction was determined by flow cytometry.

530  
531 To sort blue+ and green+ populations, 400,000 of MCF10A  $\Delta TP53$  cells (Horizon Discovery) in  
532 5 ml media plus 8 micrograms/ml polybrene were transduced at a MOI ~0.1, with either of the  
533 EGFP or EBFP expressing viruses that had been packaged singly, a mix of the EGFP and EBFP  
534 expressing viruses that had been packaged singly or the EGFP and EBFP expressing viruses that  
535 had been packaged together. The cells were then cultured for four weeks to avoid residual  
536 plasmid contamination following transduction. An equal number of cells transduced with EGFP  
537 and EBFP virus were mixed to determine the rate of contamination resulting from FACS error.

538 The mixed cells along with others were sorted for blue+ or green+ populations using a FACS  
539 Aria II (Becton Dickinson) that had been compensated for the overlap between the EBFP and  
540 EGFP emission spectra. The genomic DNA was harvested from each population using the  
541 Qiagen DNeasy kit. The barcodes were amplified from 2-36 ng of genomic DNA in 50 ul Robust  
542 polymerase (Kapa) reactions with primers bwds\_p5\_WPRE\_BC\_F and  
543 bwds\_next\_WPRE\_BC\_R.

544  
545 bwds\_next\_WPRE\_BC\_R:  
546 GGCTCGGAGATGTGTATAAGAGACAG  
547 5- gaaatcatcgtcctttccttgct -3

548  
549 bwds\_p5\_WPRE\_BC\_F:  
550 5- AATGATACGGCGACCACCGAGA ggcgccgatgccttgtaagtcattggtcttaaaggctc -3

551  
552 Reactions were removed from the thermocycler just prior to saturation (27-30 cycles). The PCR  
553 products were purified with Ampure (Agilent) and P7 index sequences were added by an  
554 additional six cycles of PCR. PCR products were purified, quantified, pooled and single-end  
555 sequenced on an Illumina Nextseq500 with Read1 primer bwds\_WPRE\_bc\_seqF and standard  
556 Illumina i7 primers.

557  
558 bwds\_WPRE\_bc\_seqF:  
559 5- GCG CCG ATG CCT TGT AAG TCA TTG GTC TTA AAG GCT CGA -3

### 560 *Analysis of FACS Data from pHAGE-GFP and pHAGE-BFP Experiments*

561 The background percentage of contaminating barcodes in the BFP/GFP sorted cells from the  
562 mixed cells control was first subtracted from the numbers obtained for the pooled virus samples.  
563 The fraction of GFP cells, as determined from FACS gating, was fixed and the expected fraction  
564 of barcode contamination in the BFP and GFP given this fixed fraction of GFP cells was  
565 simulated. Note that the expected contamination of green barcodes in the BFP sorted cells is  
566 simply the template switching rate multiplied by the fraction of green cells. The expected rate of  
567 contamination of BFP barcodes in the GFP sorted cells is simply the template switching rate  
568 multiplied by the BFP cell fraction (1 – GFP cell fraction). The sum of the squared error between  
569 the observed and expected values for these to rates of contamination was calculated for a range  
570 of different lentivirus swap rates and the minimal value was taken to be the most likely swap rate  
571 given the observed data.

572  
573 Note that, unlike in a large library of plasmids, in a mix of two plasmids, only half of all  
574 chimeric products formed will be detectable as many virions will be homozygous (contain the  
575 same construct, and thus chimeric products are identical to the original). To give an analogous



576 example, in a barnyard experiment for a single-cell assay, mouse-mouse or human-human  
577 multiplets cannot be detected and thus estimated rates of ‘doublets’ have to be adjusted  
578 accordingly. When the plasmids are equimolar and the swap rate is 50%, for example, one would  
579 expect to observe a 75% rate of the intended barcode and a 25% rate of the unintended barcode.  
580 This ratio will change according to the molar concentration of the two plasmids. In **Fig. 1f**, we  
581 assume that the pool was composed of 61.7% GFP plasmid, corresponding to the fraction of  
582 GFP+ cells relative to the total number of GFP+ and BFP+ cells --  $4.59 / (4.59 + 2.85)$  or 61.7%  
583 as explained in **Fig. S4**. This analysis was also performed without fixing the fraction of GFP+  
584 cells to the value measured by FACS to ensure results were concordant between the two methods  
585 (**Fig. S5**). The minimum sum of squared error over the grid of simulated lentivirus swap rate and  
586 fraction of GFP cells were taken to be the most likely set of parameter values.  
587

### ***CRISPRi Experiment***

588 K562 expressing dCas9-BFP-KRAB (gift of the Bassik lab, Addgene #46911) and MCF10A  
589 expressing dCas9-BFP-KRAB (made by transduction with  
590 lenti\_UCOE\_EF1-dCas9-BFP-KRAB, plamid available on Addgene soon; see  
591 <https://weissmanlab.ucsf.edu/CRISPR/CRISPRiacelllineprimer.pdf>) were transduced with  
592 lenti-mCherry under control of a CAG-promoter (pCAG\_mCherry pKH143, gift of the Bassik  
593 lab, unpublished), and sorted such that the resulting population is enriched for mCherry  
594 expression.  
595

596 A spacer targeting the CAG-promoter was cloned into the KHH030 (Addgene #89358),  
597 CROP-seq, and pHAGE sgRNA expression vectors. The CROP and pHAGE were modified by  
598 Q5-Site Directed Mutagenesis (New England BioLabs) to use the previously described  
599 sgRNA-(F+E)-combined optimized backbone<sup>28</sup>. The CRISPRi mCherry+ K562 and MCF10A  
600 cells were transduced with the CAG-targeting sgRNA, and again assayed for mCherry.  
601

602 All virus for the CRISPRi experiments were made by the Co-operative Center for Excellence in  
603 Hematology Vector Production core. All sorting was performed on a FACS Aria II (Becton  
604 Dickinson).  
605

### ***Editing Rate Experiment for pHAGE-scKO***

607 To confirm that our pHAGE-scKO vector exhibited reduced editing efficiency in addition to  
608 reduced inhibition efficiency via CRISPRi, we performed editing with a guide to TP53 from our  
609 screen (GAGCGCTGCTCAGATAGCGA) in both lentiGuide-Blast and pHAGE-scKO using our  
610 pCW-Cas9 MCF10A cells. Cells were passaged for 18 days post-induction of Cas9 expression  
611 with dox and gDNA was harvested using Qiagen DNeasy kit and amplified using primers  
612 CTAATGGCTGTGAGAGAGCTCAGCCACACGCAAATTCCTTCC and



613 ACTTTATCAATCTCGCTCCAAACCCCTGCCCTCAACAAGATGT. These were then  
614 amplified using KAPA HiFi Hotstart Ready Mix (KAPA) using the following primers to generate  
615 final indexed sequencing libraries:  
616 AATGATACGGCGACCACCGAGATCTACACacgtaggcCTAAATGGCTGTGAGAGAGCTC  
617 AG  
618  
619 CAAGCAGAAGACGGCATAACGAGAT[INDEX]gaccgtcggcACTTTATCAATCTCGCTCCA  
620 AACC  
621

622 These reads were then processed using the method described in McKenna and Findlay *et al.*<sup>29</sup>  
623 Briefly, low quality bases are trimmed using Trimmomatic, reads are merged using Flash,  
624 aligned to the reference of the locus surrounding the guide site using needle, and unique  
625 genotypes are quantified. The wild-type genotype fraction was taken to be the proportion of  
626 unedited alleles. We did not use UMIs in this experiment. The lack of UMIs may overestimate  
627 the editing rate in all samples to some extent due to amplification bias.  
628

### ***KO Experiments***

629 For all screens, each plasmid library was transfected along with plasmids provided with the  
630 ViraPower Lentiviral Expression into 293T cells. At 48 and 72 hours post transfection, viral  
631 containing supernatant were collected, filtered using a 40 µm steriflip filtration system (EMD  
632 Millipore). For arrayed experiments, individual plasmids were transfected and viruses produced  
633 as described above. For pHAGE-scKO and arrayed/pooled pLGB-scKO vector experiments,  
634 virus concentrated using Peg-it virus concentration solution (SBI). Viral titer of the concentrated  
635 lentiviral library was determined by transduction of MCF10A-Cas9 cells for 48 hours at several  
636 viral dilutions, splitting cells into replica plates, and subjecting replica plate to blasticidin.  
637 Percent control growth was used to assess MOI. MCF10A-Cas9 cells with estimated MOIs of 0.3  
638 were carried forward for further experiments.  
639

640 For pHAGE-scKO and arrayed/pooled pLGB-scKO vector experiments, media was switched to  
641 1 microgram/mL doxycycline to induce expression of Cas9 in pCW-Cas9 cells. LentiCas9-Blast  
642 cells were used for CROP-seq experiments, which do not require induction of Cas9 expression.  
643 Editing was allowed take place for 14 days for arrayed and pooled pLGB-scKO and 21 days for  
644 pHAGE-scKO and CROP-Seq experiments. Media was changed every 48 hours and cells were  
645 cultured every 96 hours. For the first half of editing, cells were cultured in the presence of 5  
646 µg/mL blasticidin and 0.5 µg/mL puromycin to ensure high sgRNA and Cas9 expression.

647

### ***Doxorubicin Treatment***

648 After editing, MCF10a cells were seeded in 10 cm plates at  $1 \times 10^6$  cells per well, allowed  
649 to attach overnight and media replaced with MCF10A media alone (mock) or MCF10A media  
650 containing 500 (arrayed and pooled pLGB-scKO experiments) or 100 nM (pHAGE-scKO and  
651 CROP-Seq experiments; we ultimately decided that this lower dose was more appropriate and  
652 likely to provide more robust signal) doxorubicin prepared from a 500  $\mu$ M stock of doxorubicin  
653 (Sigma) in water. 24 hours after drug exposure untreated and doxorubicin treated cells were  
654 harvested by trypsinization, washed with PBS and used for downstream assays.

655

### ***Single-Cell RNA-sequencing***

656 Cells were captured using one lane of a 10X Chromium device per sample using 10X V1 Single  
657 Cell 3' Solution reagents (10X Genomics). Approximately 4000-7000 cells were captured per  
658 lane for each condition. Protocols were performed according to manufacturer recommendations,  
659 holding 10-30 ng of full length cDNA out of downstream shearing and library prep steps in  
660 order to provide material for barcode enrichment PCR.

661

662 Final libraries were sequenced on NextSeq 500/550. 10X V1 samples were sequenced using the  
663 following read configuration on 75 cycle High Output kits:

664 R1: 64, R2: 5, I1: 14, I2: 8

665

666 Our initial arrayed and pooled doxorubicin treated samples using pLGB-scKO were aggregated  
667 using cellranger aggregate to normalize the average number of mapped reads per cell. This yields  
668 an average of 37,732 reads per cell, 2263 median genes per cell, and a median of 8279 UMIs per  
669 cell.

670

671 Our CROP-seq mock sample was sequenced to an average depth of 120,797 raw reads per cell in  
672 6598 cells. A median of 4619 genes per cell were detected and a median UMI count of 22,495  
673 per cell. Our CROP-seq doxorubicin treated sample was sequenced to an average depth of  
674 123,445 raw reads per cell in 6283 cells. A median of 3500 genes per cell were detected and we  
675 observed a median UMI count of 15,324 per cell. At this depth the average duplication rate is  
676 approximately 78%.

677

### ***Enrichment PCR***

678 For all experiments a hemi-nested PCR starting from 5 ng of full length cDNA was used to  
679 enrich for the barcodes that assign a target to each cell. All PCR reactions were performed with a  
680 P7 reverse primer (as introduced by the 10X Chromium V1 oligo DT RT primer). Importantly,  
681 the protocol for the 10X V2 protocol (not used here) would be different -- see

682 <https://github.com/shendurelab/single-cell-ko-screens#enrichment-pcr> for more information. For  
683 pHAGE-scKO and pLGB-scKO, the first PCR was performed with

684

685 5- TCCTGGGATCAAAGCCATAGT -3

686

687 and for CROP-Seq with

688

689 5- TTTCCCATGATTCCTTCATATTTGC -3

690

691 as the forward primer, priming to the blasticidin transcript with no non-templated sequence for  
692 pHAGE-scKO and pLGB-scKO, and to part of the U6 promoter in CROP-seq. For pLGB-scKO  
693 the second PCR was performed with

694

695 5- TCGTCGGCAGCGTCAGATGTGTATAAGAGACAGGACGAGTCGGATCTCCCTT -3

696

697 for pHAGE-scKO with

698

699 5-

700 TCGTCGGCAGCGTCAGATGTGTATAAGAGACAGAACGGACTAGCCTTATTTTAACTTG

701

-3

702

703 and for CROP-Seq with

704

705 5- TCGTCGGCAGCGTCAGATGTGTATAAGAGACAGcTTGTGGAAAGGACGAAACAC -3

706

707 as the forward primer, priming adjacent to the barcode/guide sequence in each design and adding  
708 the standard Nextera R1 primer. Samples were then indexed in a final PCR using standard  
709 Nextera P5 index primers of the form:

710

711 5- AATGATACGGCGACCACCGAGATCTACAC[8bp Index]TCGTCGGCAGCGTC -3

712

713 Each PCR was cleaned with a 1.0X Ampure XP cleanup and one microliter of a 1:5 dilution of  
714 the first PCR was carried forward and a 1:25 dilution of the second PCR was carried into the  
715 final PCR reaction. PCRs were monitored by qPCR and stopped just prior to reaching saturation  
716 to avoid overamplification. The final PCR was run on a Bioanalyzer to confirm expected product  
717 size.

718

### ***Digital Gene Expression Quantification***

719 Sequencing data from each sample was processed using cellranger 1.3.1 to generate sparse  
720 matrices of UMI counts for each gene across all cells in the experiment.

721  
722 Each lane of cells was processed independently using cellranger count, aggregating data from  
723 multiple sequencing runs. For the comparison between arrayed and pooled screens, cellranger  
724 aggregate was used to downsample data from each screen to an equal average number of mapped  
725 reads.

726

### ***Assigning Cell Genotypes***

727 Barcode enrichment libraries were separately indexed and sequenced as spike-ins alongside the  
728 whole transcriptome scRNA-seq libraries. Final UMI and cell barcode assignments were made  
729 for each read by processing these samples with cellranger 1.3.1 as was done for the whole  
730 transcriptome libraries.

731

732 A whitelist of guide or target barcode sequences was constructed using all guides or target  
733 barcodes in the library. For each read in the position sorted BAM file output by cellranger 1.3.1,  
734 the final cellular barcode and UMI are extracted. If either of these fields is not populated,  
735 indicating low sequencing quality for the cell barcode or UMI read, the read is ignored. Using  
736 the cDNA read, we attempt to find a perfect match for the sequence immediately preceding the  
737 guide or barcode (GTGGAAAGGACGAAACACCG for CROP-seq and CGCCTCCCGCG for  
738 pLGB-scKO). If a perfect match is not found, we attempt to locate the sequence in an  
739 error-tolerant manner using a striped Smith-Watterman alignment, where alignments must span a  
740 length no more than 2bp shorter than the search sequence. If a match or alignment is found, the  
741 guide or barcode sequence is extracted. If the extracted sequence does not perfectly match a  
742 whitelist sequence, we search for a matching whitelist sequence within an edit distance of half  
743 the minimum edit distance between any pair of guides or barcodes in the library (rounded down).  
744 If no match is found, the molecule is ultimately discarded. Matches to the whitelist are tracked  
745 for each cell.

746

747 We also remove likely chimeric sequences using the approach outlined in Dixit<sup>30</sup>. Briefly, within  
748 each cell, we first calculate the number of times a given UMI is observed with each observed  
749 guide assignment. We then divide these counts by the total instances of the respective UMI  
750 across all observed guide assignments within that cell. For UMI-guide assignment combinations  
751 where this fraction is less than 20%, we do not count the UMI towards the final observed guide  
752 assignment counts. While this has some impact on the raw data, we find the benefits to be  
753 modest, in contrast to results reported in Dixit *et al.*<sup>8</sup>.

754  
755 To make a set of final assignments, we take all whitelist sequences with over 10 reads and  
756 account for over 7.5% of the whitelist reads assigned to a given cell, where multiple sequences  
757 can be assigned to each cell. Whitelist sequences and their corresponding target genes are  
758 assigned to each cell. Finally, this set of assignments is merged with the filtered gene expression  
759 matrices output by cellranger such that only assignments to the set of high quality cells appear in  
760 the final dataset.

761  
762 Note that when processing CROP-seq data without PCR enrichment, we lowered the requirement  
763 for reads supporting a given guide to 3 to account for the decreased coverage of these transcripts.  
764

### 765 ***Estimation of MOI and Capture Rate***

766 The most likely multiplicity of infection and capture rate given the distribution of guide counts  
767 per cell were estimated using the generative model described in Dixit *et al.* <sup>8</sup>. Briefly, a log  
768 likelihood is calculated using a zero-truncated poisson (represents the multiplicity of infection  
769 after selection for cells that harbor a lentiviral construct) convolved with a binomial (represents  
770 the incomplete capture of transcripts containing guide sequences from cells). This model is used  
771 to to calculate log-likelihood values for a range of MOI values and capture rate values (rate of  
772 observing a guide in a cell given that the guide is present). The maximum log-likelihood is taken  
773 to be the MOI and capture rate of the experiment.  
774

### ***Removing Low Quality Cells***

775 Despite using the filtered set of cells provided by cellranger to exclude cell barcodes with low  
776 UMI counts, we consistently observed a cluster of cells with much lower UMI counts on average  
777 than the rest of the dataset when performing dimensionality reduction. To avoid including these  
778 cells in downstream analysis, we perform a simple procedure to remove any cluster with low  
779 average UMI counts.

780  
781 First, we perform PCA on the matrix of all cells and genes expressed in at least 50 cells for each  
782 condition to reduce to 12 principal components. We then reduce to a two dimensional space  
783 using tSNE. Next we perform density peak clustering in the two dimensional space using default  
784 parameters. For each cluster, we calculate the average size factor over the cluster as calculated  
785 using estimateSizeFactors in monocle2 <sup>31</sup>. We observed that filtering out clusters of cells with an  
786 average size factor of -0.85 or lower readily distinguished the low quality cluster of cells. All  
787 cells contained in these clusters were removed from downstream analysis. PCA and tSNE were  
788 performed using the monocle2 function reduceDimension with default parameters and the tSNE  
789 option. Density peak clustering was performed using the monocle2 function clusterCells.

790

### ***Simulating Loss in Power from Barcode Swapping***

791 Assignments were permuted for a fraction of cells ranging from 0 to 100% and kept fixed for the  
792 remaining fraction of cells. The monocle2 function differentialGeneTest was used to test for  
793 genes differentially expressed across the target assigned to each cell (only testing genes  
794 detectably expressed in at least 50 cells). The number of genes with a qvalue of 0.05 or lower  
795 was counted. This was performed over 10 different resamplings for each rate of swapping to  
796 obtain a distribution for each swap rate.

797  
798 The average fold-reduction in DEGs resulting from a 50% swap rate was taken to be the  
799 approximate fold change in power resulting from template switching in our original design.

800  
801 For the simulation performed on our own data, cells with a single target assignment from 100nm  
802 doxorubicin treated cells in our CROP-seq experiment were taken as the starting set of cells.

803  
804 For the simulation on data from Adamson *et al.*, processed data was obtained from GEO  
805 (GSE90546). Assignment of cells to targets were used as provided on GEO and only cells that  
806 were noted as having high quality assignment of the assigned target and noted as being a single  
807 cell were used in downstream analysis. Due to the large number of cells (50,000+) in the UPR  
808 experiment from this study and the large number of differential tests required for these  
809 simulations, the number of cells assigned to each target was downsampled by 2-fold to reduce  
810 runtime. We also performed tests on a dataset further downsampled to approximately 6,000 cells  
811 to illustrate the relationship between the initial power of a screen and the impact of simulated  
812 target swapping on sensitivity.

813

### ***tSNE Embedding Demonstrating TP53 Enriched Cluster***

814 Scaling, PCA, and tSNE on PCA results were performed with the monocle2 function  
815 reduceDimension. 20 dimensions from PCA were carried into tSNE which was performed to two  
816 dimensions using default parameters. All cells (except those excluded in the low size factor  
817 cluster) including cells with guides to multiple targets and no assigned target were included in  
818 dimensionality reduction for this plot. Percentages of cells with guides to TP53 and ARID1B  
819 were calculated including guides that contain guides to multiple targets (all cells with TP53  
820 guides were counted as TP53 cells and all cells without TP53 but with one or more guides to  
821 ARID1B were counted as ARID1B cells for the purposes of calculating reported percentages).



822

### ***Enrichment of Tumor Suppressors in Specific Molecular States***

823 Only cells containing a guide to a single target were considered in all enrichment testing. A Chi  
824 squared test was used to determine whether the distribution of individual sgRNAs and targets in  
825 tSNE space was significantly different from non-targeting controls at an FDR cutoff of 5%.  
826 Targets which did not pass this test and did not have any individual sgRNA pass the test were  
827 excluded from the subsequent enrichment tests. For each sgRNA of the remaining targets, we  
828 sought to estimate the functional editing rate (probability of a cell having a true LoF given that it  
829 received that sgRNA), but such estimates would be confounded if one accounts for the  
830 possibility of edits that cause LoF for the target gene but have incomplete penetrance on the  
831 cellular phenotype. Therefore we used an expectation maximization approach to estimate the  
832 functional edit rate of each sgRNA relative to the unknown functional edit rate of the most  
833 efficient sgRNA for a given target.

834  
835 The t-SNE cluster distribution of all cells in which a given sgRNA was detected was modeled as  
836 a mixture of the t-SNE cluster distribution of cells with a functional edit for the sgRNA's target  
837 gene and the t-SNE cluster distribution of non-targeting controls, where the mixing parameter is  
838 the relative functional edit rate for that sgRNA. In the expectation step, the t-SNE cluster  
839 distribution of cells with a functional edit for the target is estimated as the weighted average of  
840 the empirical t-SNE cluster distributions of each sgRNA for the target, weighted by the current  
841 estimates of the relative functional edit rate of the sgRNAs. In the maximization step, the relative  
842 functional edit rate of each sgRNA for the target is estimated as that which maximizes the  
843 likelihood of the observed t-SNE cluster distribution for cells receiving that sgRNA under the  
844 multinomial mixture model.

845  
846 After estimating the relative functional edit rate for each sgRNA, a weighted contingency table  
847 was constructed where the rows are targets, the columns are t-SNE clusters, and the values are  
848 weighted cell counts, where a cell's weight is proportional to the relative functional edit rate for  
849 the sgRNA it received. Fractional values were rounded down. Fisher's exact test was applied to  
850 this weighted contingency table to test for enrichment of targets amongst t-SNE clusters. Targets  
851 were defined as enriched at an FDR of 10%. Chi square and Fisher's exact test were performed  
852 using R functions `chisq.test` and `fisher.test`, respectively.

853

### ***Principal component and gene set enrichment analysis***

854 Pairwise differential gene expression analysis was performed between enriched target cells and  
855 non-targeting controls for cells in all significant enriched target-cluster pairs from our enrichment  
856 testing. The union of all differentially expressed genes across targets (FDR 5%) was used to  
857 perform principal component analysis. Gene set enrichment analysis was performed on genes



858 that had the top positive and negative loadings for principal component 1 (less than -0.02 or  
859 greater than 0.02). Gene set enrichment analysis was performed using the piano R package and  
860 the hallmarks gene set from MSigDB. Gene sets were defined as enriched at an FDR cutoff of  
861 1%. PCA was performed using the prcomp function in R, differential expression analysis was  
862 done using the monocle2 function differentialGeneTest. The hallmarks gene set collection GMT  
863 file was downloaded from the MSigDB.

864

865

866 **Figure Legends**

867

868 **Figure 1** Template switching during lentiviral packaging decreases the sensitivity of designs  
869 relying on *cis*-pairing of sgRNAs and distal barcodes. **A)** Generalized schematic of vectors that  
870 rely on *cis* pairing of sgRNAs and barcodes. **B)** Generalized schematic of CROP-seq approach.  
871 One copy of the guide is cloned into the 3' LTR of the vector and a second copy of the guide  
872 expression cassette is produced in the 5' LTR during lentivirus positive strand synthesis prior to  
873 integration. **C)** Schematic of constructs developed to quantify template switching rate at 2.4 kb  
874 separation between sequences. Distinguishing bases (3 bp differences) in GFP and BFP are  
875 separated from their respective barcodes by 2.4 kb. **D-E)** Cells were transduced with GFP or  
876 BFP virus separately or a virus generated from a mix of GFP/BFP produced from individual or  
877 combined lentiviral packaging. As an additional control, cells transduced with GFP or BFP only  
878 virus were mixed prior to sorting. Cells were sorted on GFP and BFP and the percent GFP and  
879 BFP barcodes in each sample is shown as a table. Note that in a mix of two plasmids only  
880 approximately half of all chimeric products are detectable due to homozygous virions (see  
881 Methods). **F)** Plot of sum of squared errors of observed data vs. expected values at various swap  
882 rates assuming a relative proportion of 61.7% GFP+ cells as determined from FACS (see **Fig. S4**  
883 for derivation of this percentage and the supplementary methods for a detailed explanation of  
884 how the expected values are determined). **G)** Transcription factor pilot screen from Adamson *et*  
885 *al.*, used here as a gold standard performed with arrayed lentivirus production, was subjected to  
886 simulation of progressively higher fractions of target assignment swapping to mimic the impact  
887 of template switching. Number of differentially expressed genes across the target label at FDR of  
888 5% is plotted at each swap rate. 0.5 corresponds to the 50% swap rate determined via FACS.

889

890 **Figure 2** CROP-Seq screen of tumor suppressors with high capture rate by PCR enrichment, and  
891 assessment of alternate sgRNA placement within a pol II 3'UTR . **A)** Schematic of PCR  
892 enrichment of barcoded transcripts from CROP-seq samples. **B)** Determination of the most likely  
893 multiplicity of infection and capture rate of barcoded transcripts based on a generative model. **C)**  
894 tSNE embedding of a doxorubicin treated sample with colors corresponding to cells with guides  
895 to *TP53*, cells that contain non-targeting controls (NTC), cells containing guides to non-*TP53*  
896 targets, and cells that are unassigned. **D)** *CDKN1A* and *TP53I3* expression in cells expressing  
897 either non-targeting controls or guides to *TP53*. Cells with *TP53* guides are further stratified into  
898 cells inside and outside of the *TP53* enriched cluster from panel 2C. **E)** Schematic of pHAGE  
899 design with sgRNA placed upstream of the LTR. **F)** CRISPRi knock-down of mCherry in  
900 MCF10A and K562 cells not expressing a guide (- control), KHH30 (+ control), CROP-seq, and  
901 pHAGE-scKO design. All vectors have been modified to contain a CRISPRi optimized  
902 backbone.

903  
904

905  
906 **Supplementary Figure Legends**  
907  
908 **Figure S1** Diagram of cloning protocol and barcoded transcript enrichment strategy relying on  
909 *cis* pairing of sgRNAs and barcodes (pLGB-scKO). **A)** Schematic of our final vector relying on  
910 *cis* pairing of an sgRNA and a distal barcode. **B)** Strategy for PCR enrichment of barcoded  
911 transcripts from single-cell RNA-seq data. **C)** Pooled cloning protocol. In 1.1 we start with  
912 pLentiguideBlast and digest near the final locations of the sgRNA and paired barcode. In 2.1 an  
913 engineered library of oligos containing programmed pairs of sgRNAs and corresponding  
914 barcodes are inserted into the digested vector. In 1.2 a portion of pLentiguideBlast is amplified.  
915 In 2.2 this fragment is cloned into PGEM-T. Finally, in step 3 vectors resulting from 2.1 and 2.2  
916 are digested with BsmB1 and the insert from 2.2 is ligated into the backbone in 2.1 to produce the  
917 final library of sgRNAs and paired barcodes.

918  
919 **Figure S2** Barcoded transcript enrichment quality control for arrayed and pooled pLGB-scKO  
920 experiments. Each dot represents a barcode sequence observed in a given cell. Plot of reads for a  
921 given barcode against the proportion of all barcode reads observed in a given cell for every  
922 barcode/cell pair. Red lines indicate the lower-bounds used to distinguish noise from true  
923 barcode observations (10 reads and 0.075 proportion within cell). All barcodes observed above  
924 the red lines are assigned to their respective cells. Left, doxorubicin treated sample from arrayed  
925 experiment. Right, Doxorubicin treated sample from pooled experiment.

926  
927 **Figure S3** Comparison of a screen performed with arrayed and pooled lentivirus production  
928 using a vector that relies on *cis* pairing of sgRNAs and barcodes. Experiments were performed at  
929 different times but under the same conditions. The arrayed experiment was performed as a pilot  
930 experiment with 4 targets and observed an overall low rate of cells with detected barcodes. The  
931 pooled experiment was performed afterwards with 10 targets and a set of non-targeting controls  
932 and we observed a high proportion of cells with detected barcodes and good coverage of the  
933 library. To compare these experiments, only the four overlapping targets were considered and the  
934 number of cells containing an sgRNA to each target and sequencing depth were matched  
935 between samples to control for power differences. **A)** Size-factor normalized *CDKN1A* and  
936 *TP53I3* expression across *TP53* and the three other targets in arrayed screen. **B)** *CDKN1A* and  
937 *TP53I3* expression across *TP53* and three other targets in pooled screen that overlap with the  
938 arrayed screen. **C)** Comparison of the number of differentially expressed genes detected at an  
939 FDR of 5% for arrayed across the target label in the arrayed and pooled experiments.

940  
941  
942  
943

944  
945 **Figure S4** Design and sorting of GFP and BFP positive fractions in lentivirus barcode swapping  
946 experiment. **A)** Schematic of vectors (pHAGE-GFP and pHAGE-BFP) designed to quantify  
947 template switching rate at 2.4 kb using a FACS readout. FACS plots are shown for sorted cells in  
948 samples corresponding to **B)** GFP only transduced cells **C)** BFP only transduced cells **D)** GFP  
949 and BFP only transduced cells mixed just prior to FACS as a control **E)** cells transduced with  
950 BFP and GFP virus that was generated separately but pooled prior to transduction **F)** cells  
951 transduced with BFP and GFP virus that was generated from pooled plasmids. The fraction of  
952 green plasmids assumed in the determination of lentivirus swap rate from FACS experiments is  
953 taken as the fraction of GFP+ cells relative to the total GFP+ and BFP+ cells from this sort ( $4.59$   
954  $/ (4.59 + 2.85)$  or 61.7%). This accounts for the fact that plasmids were likely not completely  
955 equimolar. The approximate number of total cells sorted in each fraction is indicated along  
956 the appropriate axes on each plot.

957  
958  
959 **Figure S5** Simulation of concordance between observed and expected data obtained from FACS  
960 experiment in **Fig. S4** to quantify template switching rate at 2.4 kb separation between paired  
961 sequences. **Fig. 1F** assumed a fraction of 0.617 of GFP plasmid in the original green plasmid /  
962 blue plasmid mix as determined from FACS in **Fig. S5**. In this figure, both the fraction of GFP  
963 plasmid and lentivirus swap rate are varied to obtain the set of parameters that best fit the  
964 collected data. The sum of the squared error between expected and observed values from FACS  
965 given each combination of parameters is shown.

966  
967 **Figure S6** Guide transcript enrichment quality control plot for tumor suppressor knock-out  
968 screen performed with CROP-seq. Each dot represents a guide sequence observed in a given cell.  
969 Plot of reads for a given guide against the proportion of all guide reads observed in a given cell  
970 for every barcode/cell pair. Red lines indicate the lower-bounds used to distinguish noise from  
971 true guide observations (10 reads and 0.075 proportion within cell). All guide observed above the  
972 red lines are assigned to their respective cells. Left, Doxorubicin treated sample from CROP-seq  
973 experiment. Right, Mock sample from CROP-seq experiment.

974  
975  
976  
977  
978  
979  
980  
981  
982

983 **Figure S7** Loss of several targets alter the distribution of mock and doxorubicin exposed cells  
984 within tSNE clusters. **A-B)** 3D tSNE embedding and clustering of mock and doxorubicin treated  
985 samples, respectively. **C-F)** Chi-squared test qvalues (p values adjusted using the  
986 Benjamini-Hochberg method) resulting from testing for differences in the distribution of targets  
987 in our screen at both the individual sgRNA (**C and E**) and overall target levels (**D and F**).  
988 Comparisons are relative to the distribution of non-targeting controls across tSNE clusters for  
989 mock and doxorubicin treated samples, respectively (qvalues were capped to  $1e-50$  for  
990 visualization). Significant differences below a qvalue of 0.05 are colored in red (boundary  
991 marked by the grey dashed line).

992  
993 **Figure S8** Enriched target-cluster pairs highlight tumor suppressors that share various degrees of  
994 a *TP53* deficient signature **A)** Fisher's exact with weights applied to guides according to an  
995 expectation maximization procedure were performed for the doxorubicin treated sample to find  
996 clusters from Fig. S7 panel B were particular targets were found to be enriched. Cells with  
997 target-cluster pairs that showed enrichment were used to generate an aggregate expression profile  
998 for every target within genes that are differentially expressed between *TP53* and non targeting  
999 controls (NTC). A PCA was performed on these average expression profiles and a distribution of  
1000 targets across PC1 is shown colored by the cluster in which they were found to be enriched. **B)**  
1001 Gene set enrichments for top positively and negatively loaded (less than -0.02 or greater than  
1002 0.02) genes along PC1 (qval < 0.01). **C)** Differential expression tests were performed for cells  
1003 within each enriched target-cluster pair, comparing each target to all NTC cells. The proportion  
1004 of overlap between these differentially expressed genes and the genes differentially expressed  
1005 between *TP53* and NTC is shown.

1006  
1007 **Figure S9** Swap rate simulations for our own CROP-seq tumor suppressor screen and the  
1008 unfolded protein response screen from Adamson *et al.* Each dataset was subjected to simulation  
1009 of progressively higher fractions of target assignment swapping to mimic the impact of template  
1010 switching. Number of differentially expressed genes across the target label at FDR of 5% is  
1011 plotted at each swap rate. 0.5 corresponds to the 50% swap rate determined via FACS. **A)**  
1012 CROP-seq tumor suppressor screen from our study. **B)** Unfolded protein response screen from  
1013 Adamson *et al.* downsampled from ~50,000 to 25,000 cells to make simulations computationally  
1014 feasible. **C)** Unfolded protein response screen from Adamson *et al.* downsampled to 6,000 cells  
1015 to illustrate how reduced power impacts the observed impact from simulated swapping.

1016

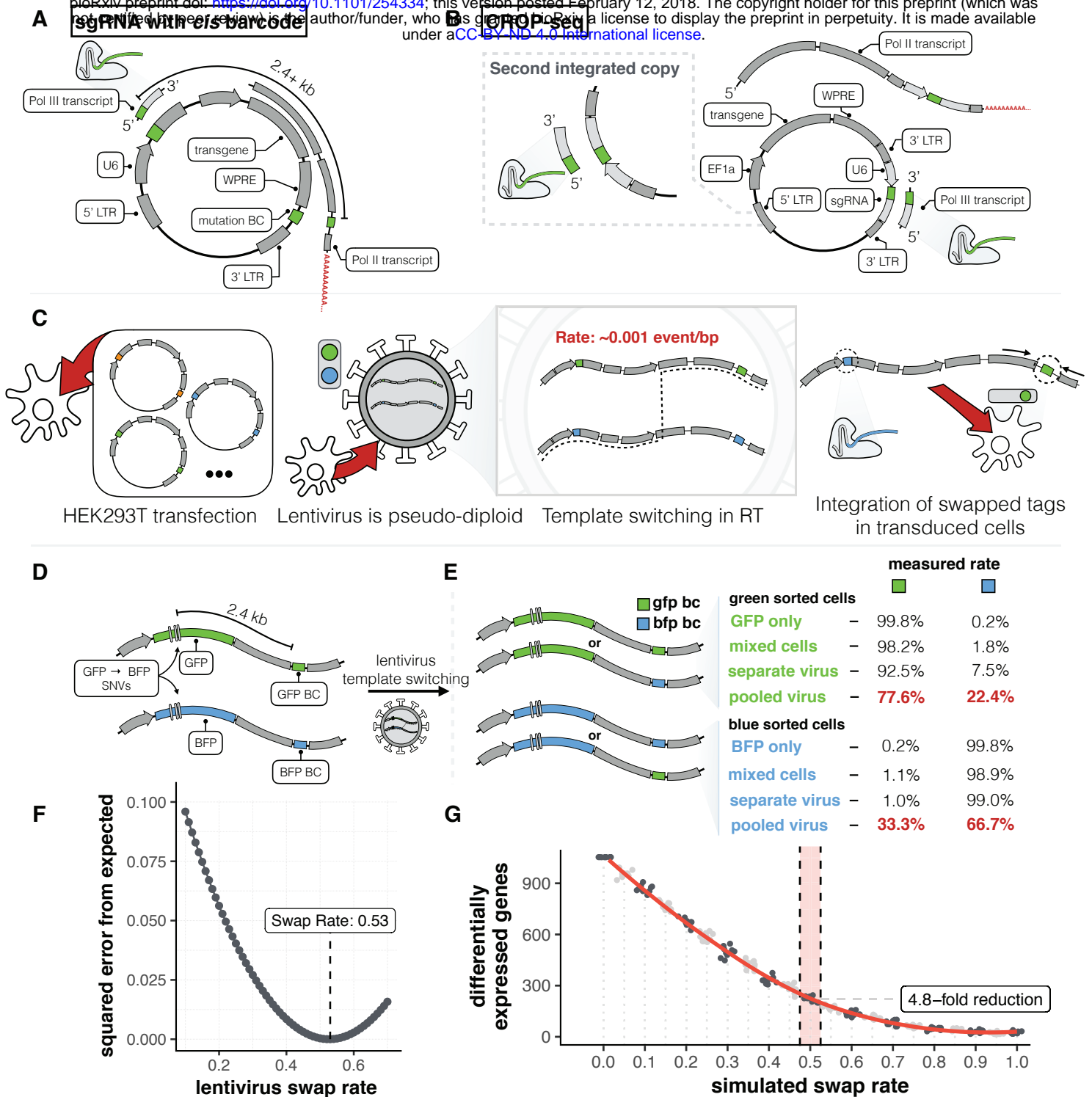


**Figure 1** Template switching during lentiviral packaging decreases the sensitivity of designs relying on cis-pairing of sgRNAs and distal barcodes. **A)** Generalized schematic of vectors that rely on *cis* pairing of sgRNAs and barcodes. **B)** Generalized schematic of CROP-seq approach. One copy of the guide is cloned into the 3' LTR of the vector and a second copy of the guide expression cassette is produced in the 5' LTR during lentivirus positive strand synthesis prior to integration. **C)** Schematic of constructs developed to quantify template switching rate at 2.4 kb separation between sequences. Distinguishing bases (3 bp differences) in GFP and BFP are separated from their respective barcodes by 2.4 kb. **D-E)** Cells were transduced with GFP or BFP virus separately or a virus generated from a mix of GFP/BFP produced from individual or combined lentiviral packaging. As an additional control, cells transduced with GFP or BFP only virus were mixed prior to sorting. Cells were sorted on GFP and BFP and the percent GFP and BFP barcodes in each sample is shown as a table. Note that in a mix of two plasmids only approximately half of all chimeric products are detectable. **F)** Plot of sum of squared errors of observed data vs. expected values at various swap rates assuming a relative proportion of 61.7% GFP+ cells as determined from FACS (see **Fig. S4** for derivation of this percentage and the supplementary methods for a detailed explanation of how the expected values are determined). **G)** Transcription factor pilot screen from Adamson *et al.*, used here as a gold standard, was subjected to simulation of progressively higher fractions of target assignment swapping to mimic the impact of template switching. Number of differentially expressed gene across the target label at FDR of 5% is plotted at each swap rate. 0.5 corresponds to the 50% swap rate determined via FACS.



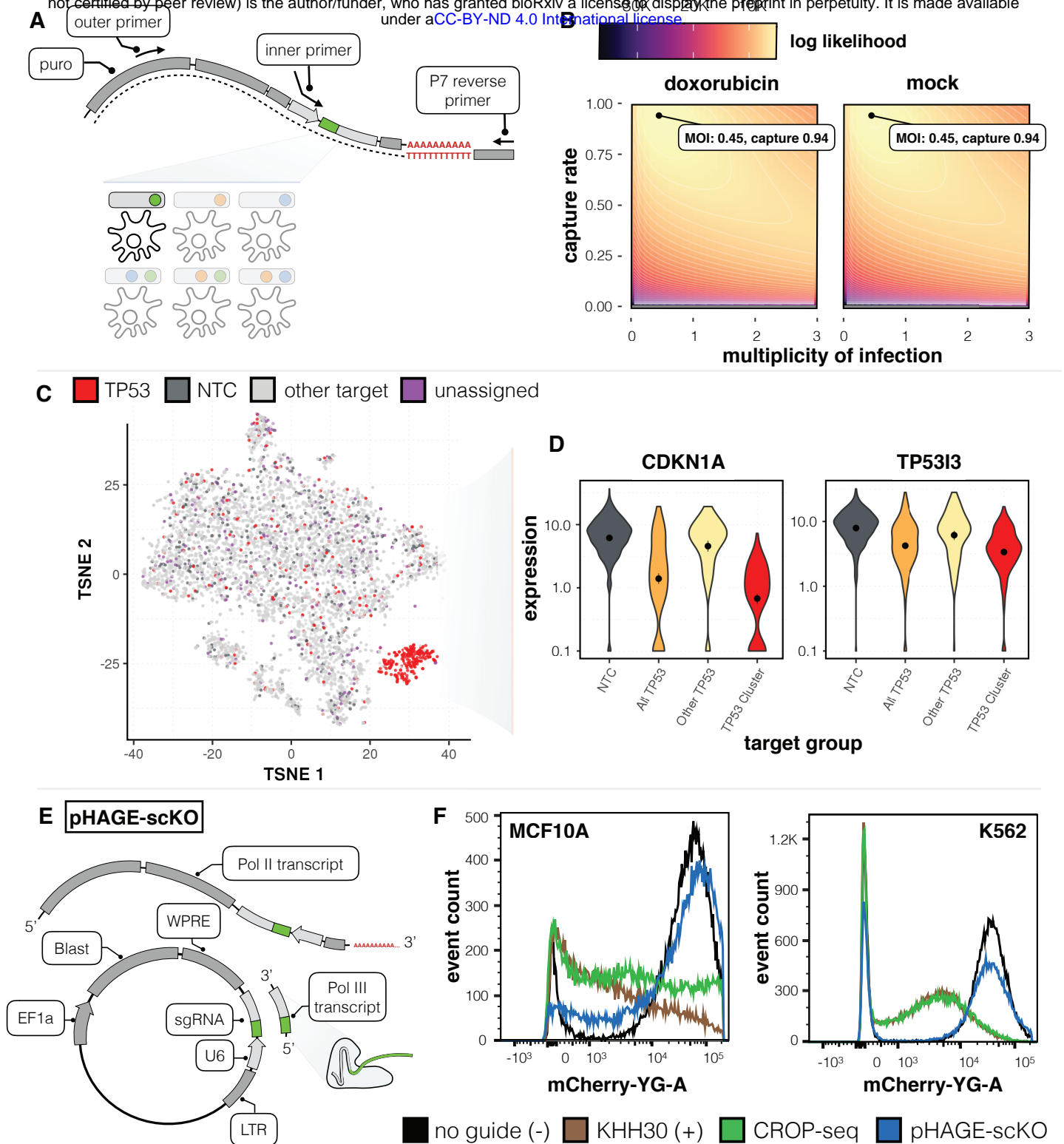


**Figure 2** CROP-Seq screen of tumor suppressors with high capture rate by PCR enrichment, and assessment of alternate sgRNA placement within a pol II 3'UTR . **A)** Schematic of PCR enrichment of barcoded transcripts from CROP-seq samples. **B)** Determination of the most likely multiplicity of infection and capture rate of barcoded transcripts based on a generative model. **C)** tSNE embedding of a doxorubicin treated sample with colors corresponding to cells with guides to *TP53*, cells that contain non-targeting controls (NTC), cells containing guides to non-*TP53* targets, and cells that are unassigned. **D)** *CDKN1A* and *TP53I3* expression in cells expressing either non-targeting controls or guides to *TP53*. Cells with *TP53* guides are further stratified into cells inside and outside of the *TP53* enriched cluster from panel 2C. **E)** Schematic of pHAGE design with sgRNA placed upstream of the LTR. **F)** CRISPRi knock-down of mCherry in MCF10A and K562 cells not expressing a guide (- control), KHH30 (+ control), CROP-seq, and pHAGE-scKO design. All vectors contain a CRISPRi optimized backbone in this experiment.



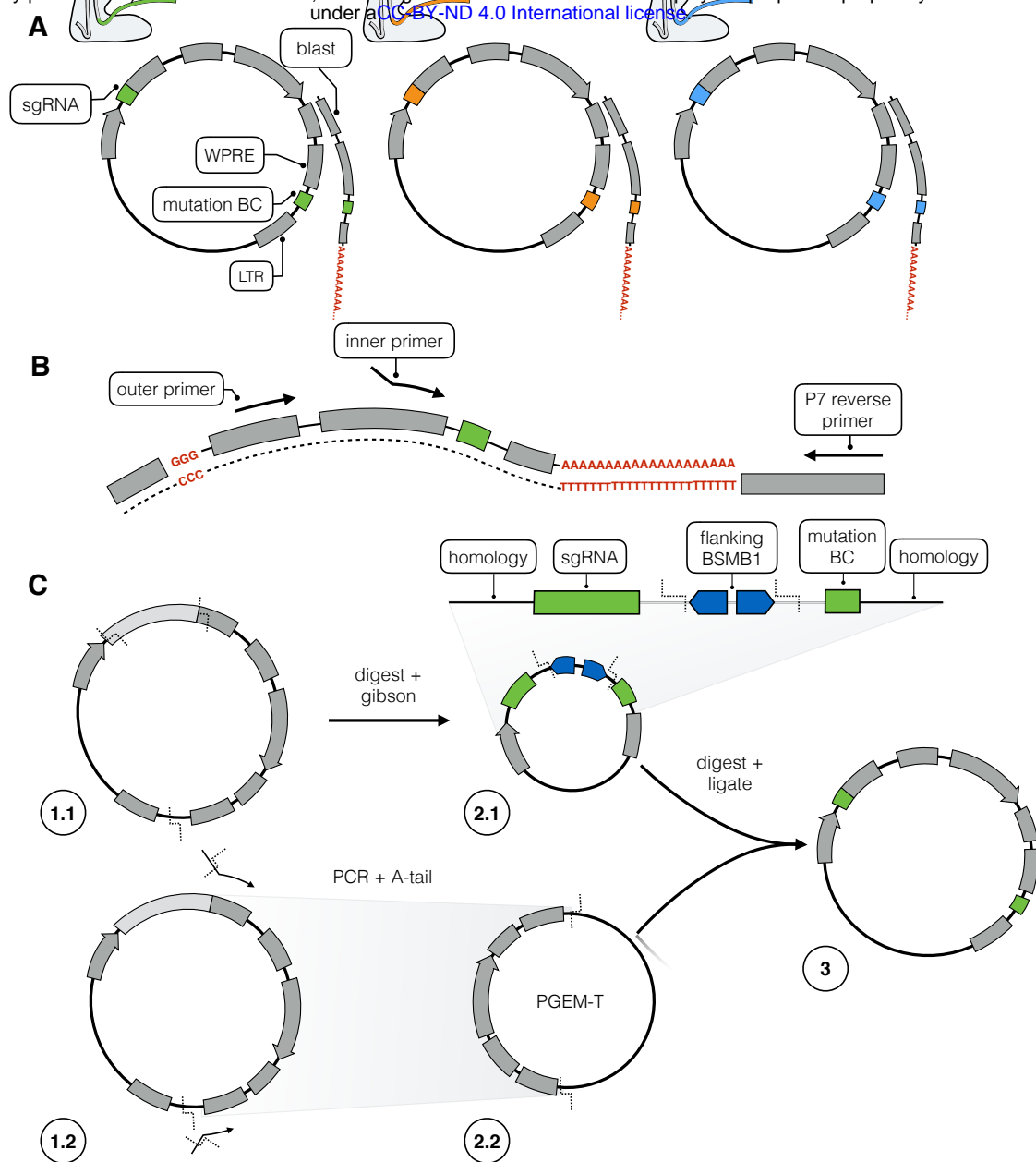


**Figure S1** Diagram of cloning protocol and barcoded transcript enrichment strategy relying on *cis* pairing of sgRNAs and barcodes (pLGB-scKO). **A)** Schematic of our final vector relying on *cis* pairing of an sgRNA and a distal barcode. **B)** Strategy for PCR enrichment of barcoded transcripts from single-cell RNA-seq data. **C)** Pooled cloning protocol. In 1.1 we start with pLentiguideBlast and digest near the final locations of the sgRNA and paired barcode. In 2.1 an engineered library of oligos containing programmed pairs of sgRNAs and corresponding barcodes are inserted into the digested vector. In 1.2 a portion of pLentiguideBlast is amplified. In 2.2 this fragment is cloned into PGEM-T. Finally, in step 3 vectors resulting from 2.1 and 2.2 are digested with Bsmbl and the insert from 2.2 is ligated into the backbone in 2.1 to produce the final library of sgRNAs and paired barcodes.

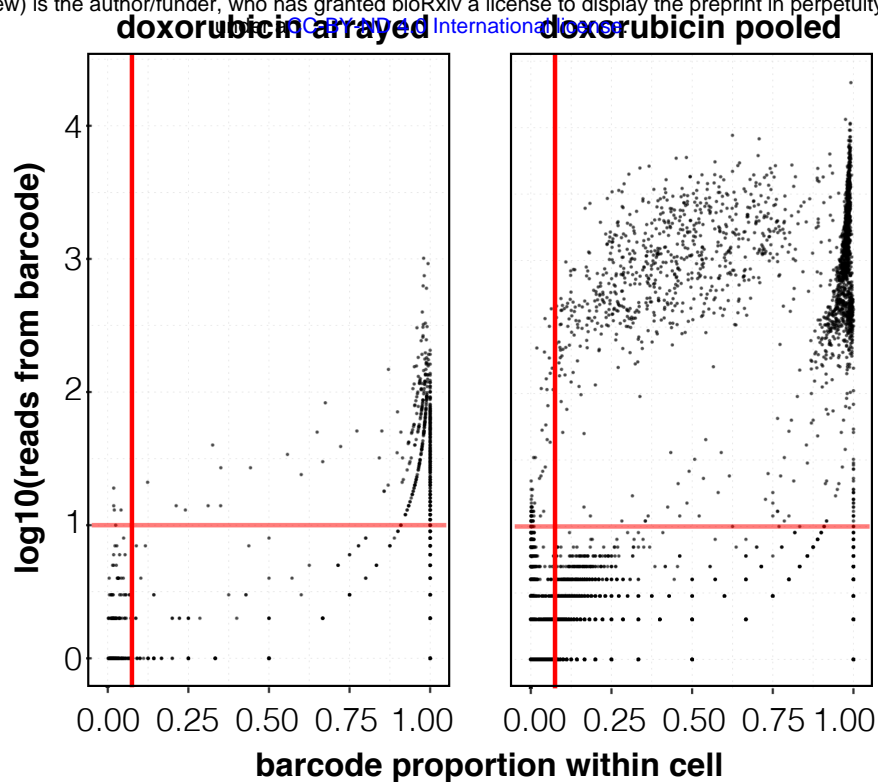


**Figure S2** Barcoded transcript enrichment quality control for arrayed and pooled pLGB-scKO experiments. Each dot represents a barcode sequence observed in a given cell. Plot of reads for a given barcode against the proportion of all barcode reads observed in a given cell for every barcode/cell pair. Red lines indicate the lower-bounds used to distinguish noise from true barcode observations (10 reads and 0.075 proportion within cell). All barcodes observed above the red lines are assigned to their respective cells. Left, doxorubicin treated sample from arrayed experiment. Right, Doxorubicin treated sample from pooled experiment.

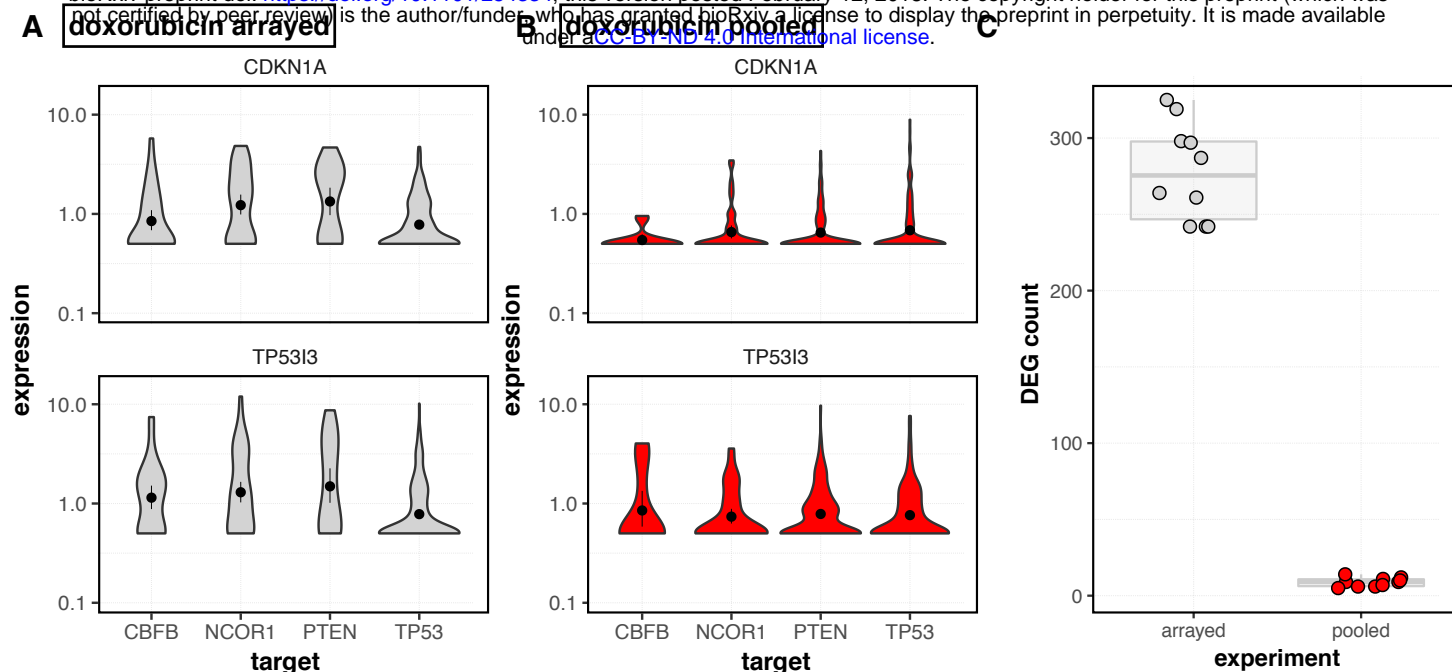


**Figure S3** Comparison of a screen performed with arrayed and pooled lentivirus production using a vector that relies on *cis* pairing of sgRNAs and barcodes. Experiments were performed at different times but under the same conditions. The arrayed experiment was performed as a pilot experiment with 4 targets and observed an overall low rate of cells with detected barcodes. The pooled experiment was performed afterwards with 10 targets and a set of non-targeting controls and we observed a high proportion of cells with detected barcodes and good coverage of the library. To compare these experiments, only the four overlapping targets were considered and the number of cells containing an sgRNA to each target and sequencing depth were matched between samples to control for power differences. **A)** Size-factor normalized *CDKN1A* and *TP53I3* expression across *TP53* and the three other targets in arrayed screen. **B)** *CDKN1A* and *TP53I3* expression across *TP53* and three other targets in pooled screen that overlap with the arrayed screen. **C)** Comparison of the number of differentially expressed genes detected at an FDR of 5% for arrayed across the target label in the arrayed and pooled experiments.

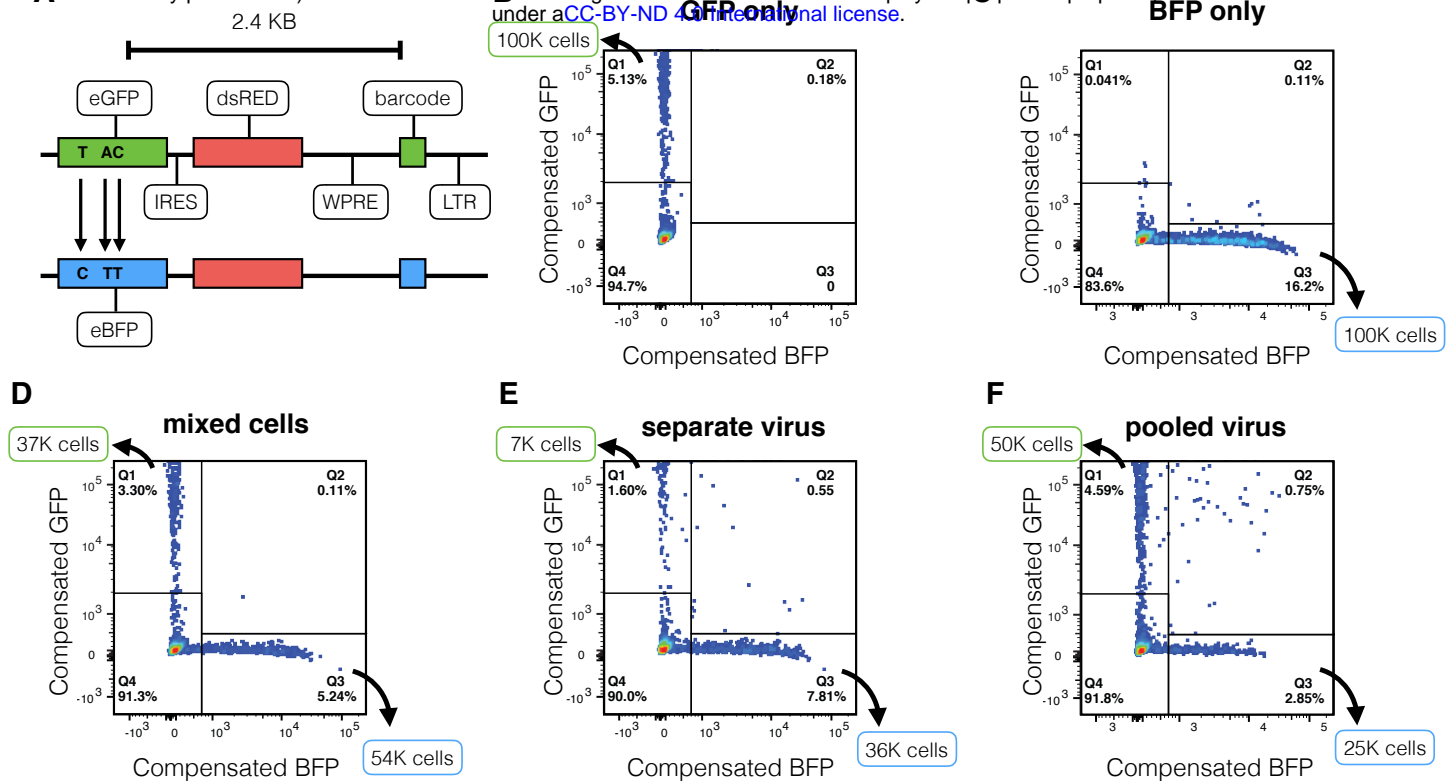


**Figure S4** Design and sorting of GFP and BFP positive fractions in lentivirus barcode swapping experiment. **A**) Schematic of vectors (pHAGE-GFP and pHAGE-BFP) designed to quantify template switching rate at 2.4 kb using a FACS readout. FACS plots are shown for sorted cells in samples corresponding to **B**) GFP only transduced cells **C**) BFP only transduced cells **D**) GFP and BFP only transduced cells mixed just prior to FACS as a control **E**) cells transduced with BFP and GFP virus that was generated separately but pooled prior to transduction **F**) cells transduced with BFP and GFP virus that was generated from pooled plasmids. The fraction of green plasmids assumed in the determination of lentivirus swap rate from FACS experiments is taken as the fraction of GFP+ cells relative to the total GFP+ and BFP+ cells from this sort ( $4.59 / (4.59 + 2.85)$  or 61.7%). This accounts for the fact that plasmids were likely not completely equimolar. The approximate number of total cells sorted in each fraction is indicated along the appropriate axes on each plot.

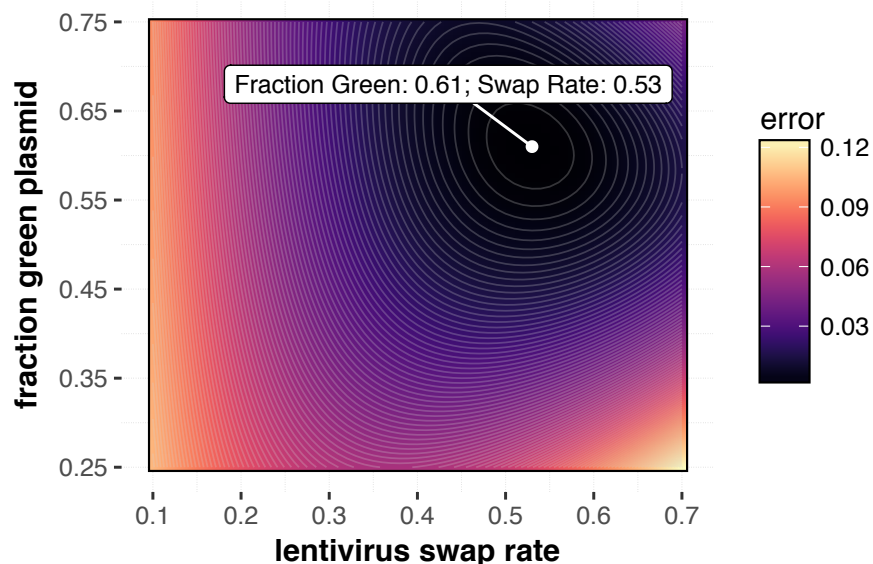


**Figure S5** Simulation of concordance between observed and expected data obtained from FACS experiment in **Fig. S4** to quantify template switching rate at 2.4 kb separation between paired sequences. **Fig. 1F** assumed a fraction of 0.617 of GFP plasmid in the original green plasmid / blue plasmid mix as determined from FACS in **Fig. S5**. In this figure, both the fraction of GFP plasmid and lentivirus swap rate are varied to obtain the set of parameters that best fit the collected data. The sum of the squared error between expected and observed values from FACS given each combination of parameters is shown.

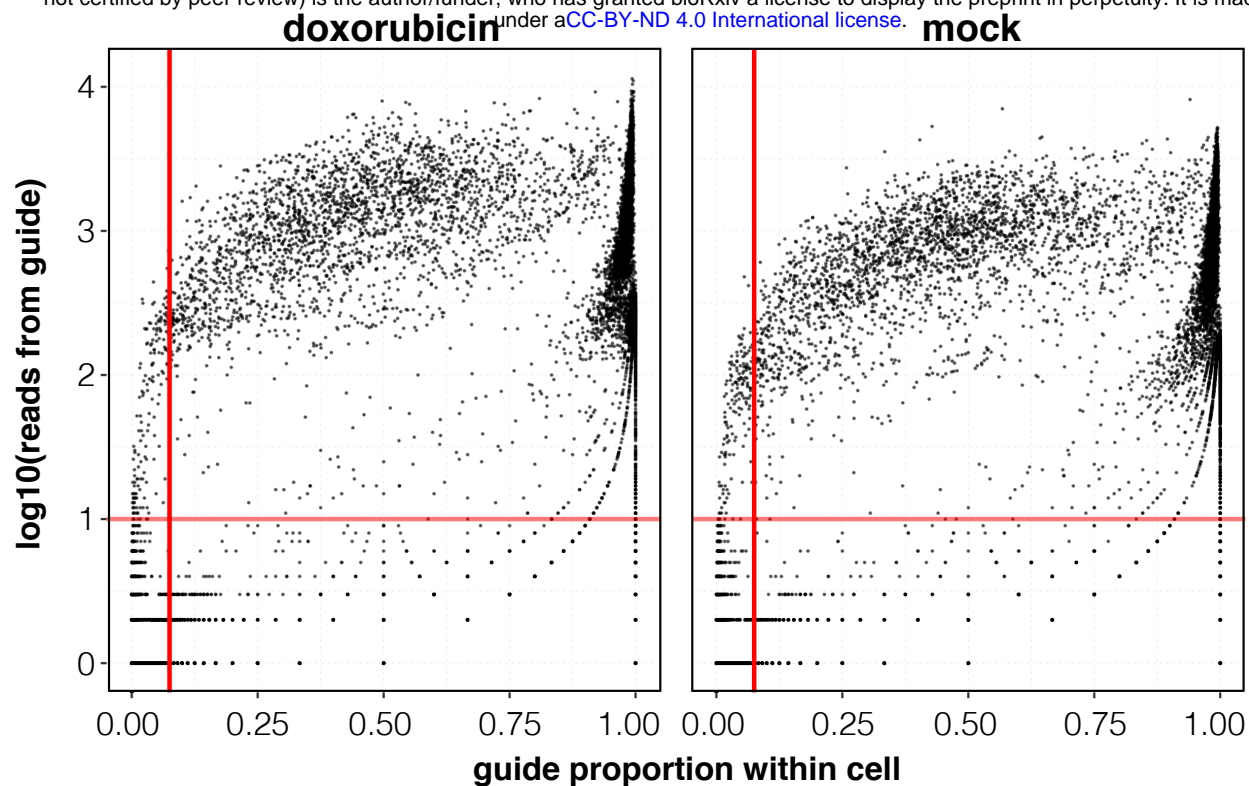


**Figure S6** Guide transcript enrichment quality control plot for tumor suppressor knock-out screen performed with CROP-seq. Each dot represents a guide sequence observed in a given cell. Plot of reads for a given guide against the proportion of all guide reads observed in a given cell for every barcode/cell pair. Red lines indicate the lower-bounds used to distinguish noise from true guide observations (10 reads and 0.075 proportion within cell). All guide observed above the red lines are assigned to their respective cells. Left, Doxorubicin treated sample from CROP-seq experiment. Right, Mock sample from CROP-seq experiment.



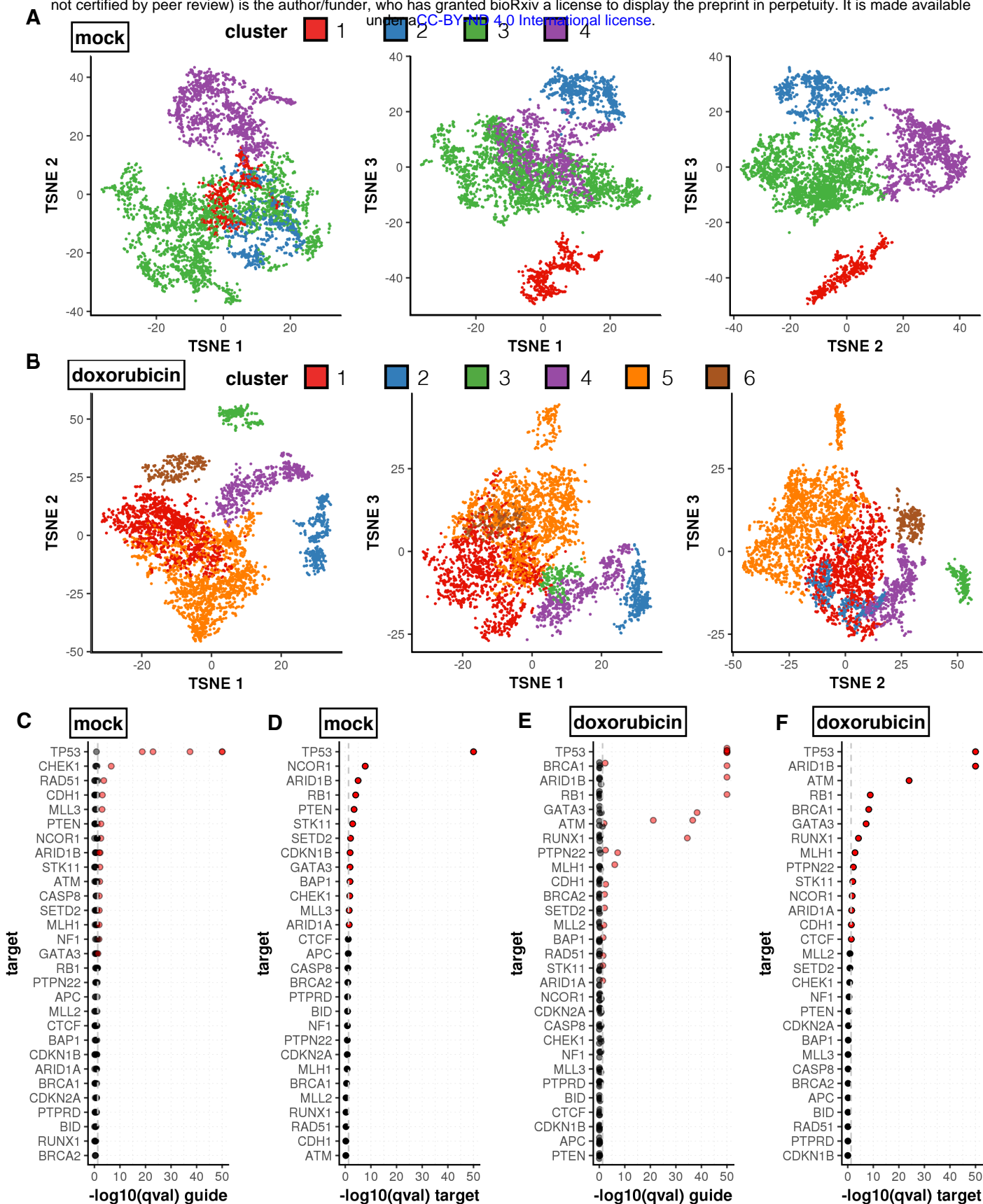
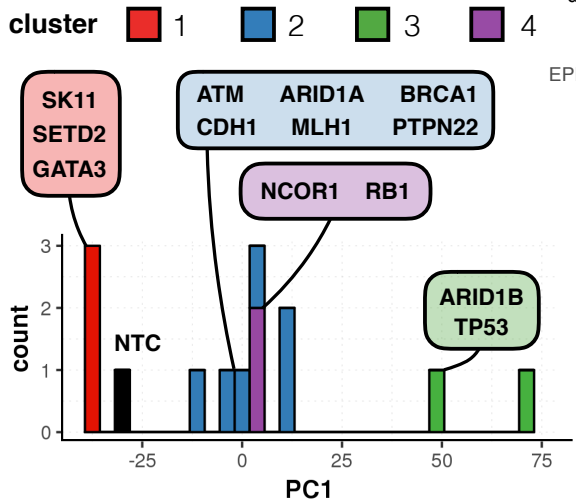
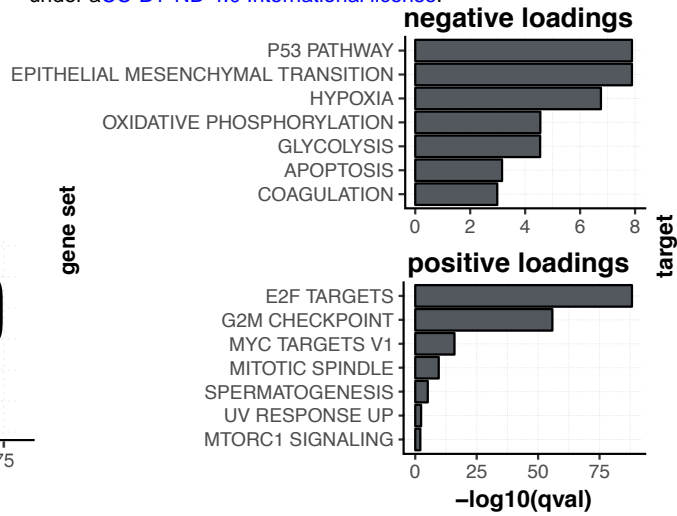


**Figure S7** Loss of several targets alter the distribution of mock and doxorubicin exposed cells within tSNE clusters. **A-B)** 3D tSNE embedding and clustering of mock and doxorubicin treated samples, respectively. **C-F)** Chi-squared test qvalues (p values adjusted using the Benjamini-Hochberg method) resulting from testing for differences in the distribution of targets in our screen at both the individual sgRNA (**C and E**) and overall target levels (**D and F**). Comparisons are relative to the distribution of non-targeting controls across tSNE clusters for mock and doxorubicin treated samples, respectively (qvalues were capped to  $1e-50$  for visualization). Significant differences below a qvalue of 0.05 are colored in red (boundary marked by the grey dashed line).

**A**



**B**



**C**

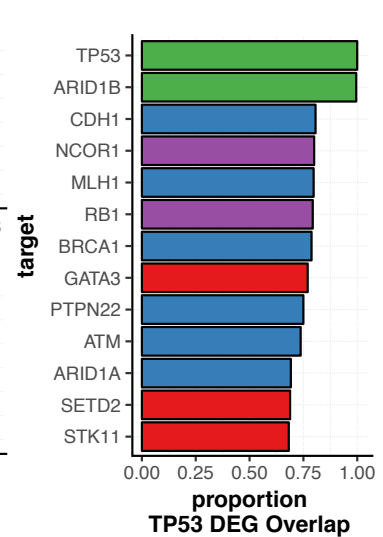


**Figure S8** Enriched target-cluster pairs highlight tumor suppressors that share various degrees of a *TP53* deficient signature **A)** Fisher's exact with weights applied to guides according to an expectation maximization procedure were performed for the doxorubicin treated sample to find clusters from Fig. S7 panel B were particular targets were found to be enriched. Cells with target-cluster pairs that showed enrichment were used to generate an aggregate expression profile for every target within genes that are differentially expressed between *TP53* and non targeting controls (NTC). A PCA was performed on these average expression profiles and a distribution of targets across PC1 is shown colored by the cluster in which they were found to be enriched. **B)** Gene set enrichments for top positively and negatively loaded (less than -0.02 or greater than 0.02) genes along PC1 ( $q_{val} < 0.01$ ). **C)** Differential expression tests were performed for cells within each enriched target-cluster pair, comparing each target to all NTC cells. The proportion of overlap between these differentially expressed genes and the genes differentially expressed between *TP53* and NTC is shown.

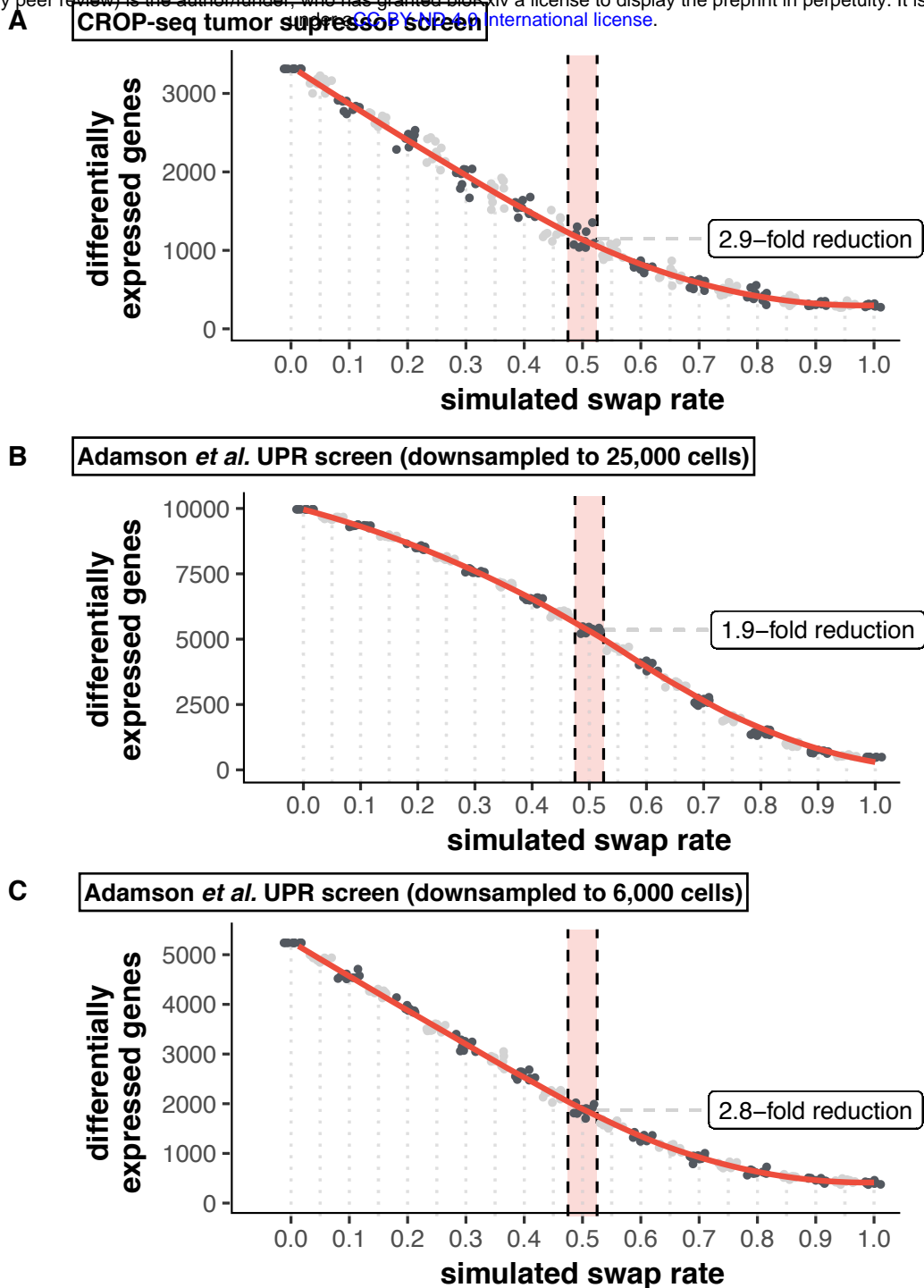


**Figure S9** Swap rate simulations for our own CROP-seq tumor suppressor screen and the unfolded protein response screen from Adamson *et al.* Each dataset was subjected to simulation of progressively higher fractions of target assignment swapping to mimic the impact of template switching. Number of differentially expressed genes across the target label at FDR of 5% is plotted at each swap rate. 0.5 corresponds to the 50% swap rate determined via FACS. **A)** CROP-seq tumor suppressor screen from our study. **B)** Unfolded protein response screen from Adamson *et al.* downsampled from ~50,000 to 25,000 cells to make simulations computationally feasible. **C)** Unfolded protein response screen from Adamson *et al.* downsampled to 6,000 cells to illustrate how reduced power impacts the observed impact from simulated swapping.